

## REVIEW

[View Article Online](#)  
[View Journal](#) | [View Issue](#)



Cite this: *Nanoscale Adv.*, 2022, **4**, 4447

## Antibacterial lignin-based nanoparticles and their use in composite materials

A. Gala Morena and Tzanko Tzanov \*

Lignin, one of the most abundant biopolymers on earth, has been traditionally considered a low-value by-product of the pulp and paper industries. This renewable raw material, besides being a source of valuable molecules for the chemical industry, also has antioxidant, UV-absorbing, and antibacterial properties in its macromolecular form. Moreover, lignin in the form of nanoparticles (LigNPs) presents advantages over bulk lignin, such as higher reactivity due to its larger surface-to-volume ratio. In view of the rapid surge of antimicrobial resistance (AMR), caused by the overuse of antibiotics, continuous development of novel antibacterial agents is needed. The use of LigNPs as antibacterial agents is a suitable alternative to conventional antibiotics for topical application or chemical disinfectants for surfaces and packaging. Besides, their multiple and unspecific targets in the bacterial cell may prevent the emergence of AMR. This review summarizes the latest developments in antibacterial nano-formulated lignin, both in dispersion and embedded in materials. The following roles of lignin in the formulation of antibacterial NPs have been analyzed: (i) an antibacterial active in nanoformulations, (ii) a reducing and capping agent for antimicrobial metals, and (iii) a carrier of other antibacterial agents. Finally, the review covers the inclusion of LigNPs in films, fibers, hydrogels, and foams, for obtaining antibacterial lignin-based nanocomposites for a variety of applications, including food packaging, wound healing, and medical coatings.

Received 29th June 2022  
Accepted 19th September 2022

DOI: 10.1039/d2na00423b  
[rsc.li/nanoscale-advances](http://rsc.li/nanoscale-advances)

### 1. Introduction

Lignocellulosic biomass is an abundant renewable resource considered a suitable carbon raw material for the synthesis of chemicals<sup>1</sup> and as an energy supply source alternative to fossil



Angela Gala Morena is a PhD candidate under the supervision of Prof. Tzanko Tzanov at the Molecular and Industrial Biotechnology Group (GBMI) of the Polytechnic University of Catalonia, Spain. She obtained her Bachelor's degree in Biotechnology (2016) and Master's degree in Advanced Microbiology (2017) at the University of Barcelona, Spain. Her current research is focused

on the synthesis and functionalization of antibacterial lignin nanoparticles and development of lignin-based materials for industrial and biomedical applications.



Prof. Tzanko Tzanov is the leader of the GBMI group and a Professor at the Polytechnic University of Catalonia, Spain. He has broad internationally acquired experience in biochemical functionalization of polymers, bioremediation of industrial effluents, enzymatic synthesis, polymerization and coating. He has been participating in numerous industry-driven European research projects in the areas of applied biotechnology, nanotechnology and health, and several national and industry-funded projects. Prof. Tzanov's scientific excellence has been recognized with the ICREA Academia 2021 award. He is the author of more than 100 peer-reviewed papers and 12 patents in the areas of materials and applied biotechnology.



fuels.<sup>2</sup> Cellulose, hemicellulose, and lignin are the primary components of lignocellulosic biomass, among which lignin represents from 15 to 30% of its dry mass in woody plants.<sup>3,4</sup> Lignin, the most abundant aromatic molecule on earth, has been traditionally considered a low value by-product of paper manufacturing. Around 70 million tons of lignin are generated as a by-product by the pulp and paper industry,<sup>5</sup> whereof only 2–5% is used in its macromolecular form.<sup>6</sup> Its underutilization is mainly due to the heterogeneous molecular structure of lignin, which highly depends on the extraction and purification methods, in addition to its low compatibility with polymeric matrices in composite production. In recent years, the potential of lignin for the synthesis of value-added materials has been considered in various fields. Lignin is rich in a variety of functional groups, including phenolic and aliphatic hydroxyl, carboxylic, carbonyl, and methoxyl groups, which provide this biopolymer with antibacterial, antioxidant, and UV-blocking capacities.<sup>6,7</sup> Nanotransformation of lignin yields nano-entities with higher reactivity compared to their bulk counterparts, whose inclusion in composites endows them with enhanced mechanical properties and bioactivities.<sup>8</sup> Nano-formulation of lignin is an emerging valorization approach, yielding lignin nanoparticles (LigNPs) that have been used as mechanical reinforcement in polymeric matrices,<sup>9</sup> as UV absorbents,<sup>10</sup> antibacterial and antioxidant agents in food packaging,<sup>11</sup> and as carriers for drug delivery.<sup>12</sup> Recent reviews address the bioactivities of macromolecular lignin<sup>13,14</sup> in biomedical applications,<sup>15</sup> the methods for the synthesis of LigNPs<sup>16–21</sup> and their different applications,<sup>22–26</sup> and the combination of lignin with other materials or actives to obtain hybrid nanocomposites.<sup>27</sup>

In light of the rapid surge of antimicrobial resistance (AMR), driven by the misuse and overuse of antibiotics, research has been focused on developing novel antimicrobials for substituting conventional antibiotics. The use of LigNPs as antibacterial agents is a suitable alternative to traditional antibiotics owing to their antibacterial properties and their biocompatibility, coupled with additional bioactivities such as antioxidant and UV-blocking properties. In view of the increasing interest in LigNPs for advanced antibacterial applications, in this review we attempt to summarize the latest developments in nano-formulated lignin with antibacterial properties. The different roles of lignin in the synthesis of nano-enabled antibacterial agents could be outlined as: (i) an antibacterial active in nanoformulations, (ii) a reducing and

capping agent for antimicrobial metals, metalloids, and metal oxides, and (iii) a carrier of antibacterial agents. The possible antibacterial mechanisms of action of lignin and LigNPs will also be discussed. This review covers different antibacterial lignin-based nanocomposite materials for a variety of applications, including food packaging, wound healing, and medical coatings among others. We aim to highlight the advantages of using a natural-based, renewable, biocompatible, and multi-functional polymer for the synthesis of nano-enabled antibacterial agents with enhanced efficacy.

## 2. Occurrence, structure, extraction, and bioactivities of lignin

### 2.1. Lignin in plants

Lignin is found in the secondary cell wall and in the middle lamella of vascular plants.<sup>28</sup> Lignin and hemicellulose encase the cellulose fibrils, providing mechanical support to the plant and allowing water conduction (Fig. 1). Besides its structural role, the polyphenolic composition of lignin and its hydrophobic nature ensure the resistance of plants to biological and chemical degradation,<sup>29</sup> and assists in their defense against pathogens.<sup>30</sup>

The content of lignin differs between plants and varies depending on the tissue, location in the cell, and the environmental conditions. For instance, hardwood and softwood plants are lignin-rich, containing 16–24 and 25–31% of lignin, respectively, while herbaceous plants such as hemp and cotton, present low contents (~6%) of this polymer. The major component of coir fibers in coconut husk is lignin (43–49%), in contrast to lower amounts found in other parts of the plant.<sup>4</sup>

### 2.2. Lignin structure and biosynthesis

The chemical structure, molecular weight, functional groups, and properties of lignin highly depend on the origin and the extraction method. The complex nature and low solubility of native lignin provoke inherent difficulties in its analysis, which hampers the development of an accurate structural model.<sup>31</sup> Lignins isolated by enzymatic digestion (cellulolytic enzyme lignin, CEL) and by ball milling (milled wood lignin, MWL) followed by dioxane extraction are considered the most representative of native lignins since these processes minimize the structural changes and increase the solubility of the molecule.<sup>32</sup>

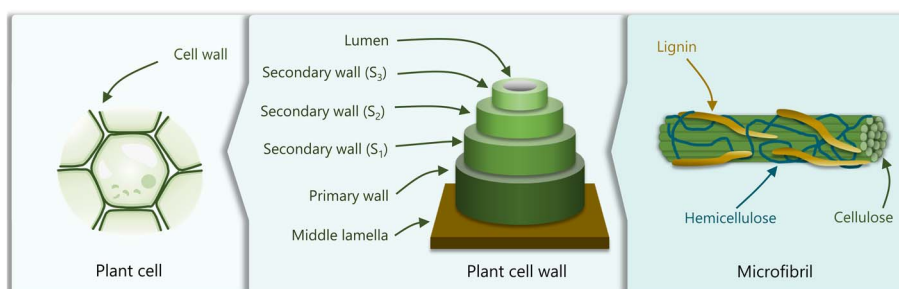


Fig. 1 Schematic representation of the cellular plant structure, comprising plant cells, the cell wall, and microfibrils. Adapted from ref. 22.



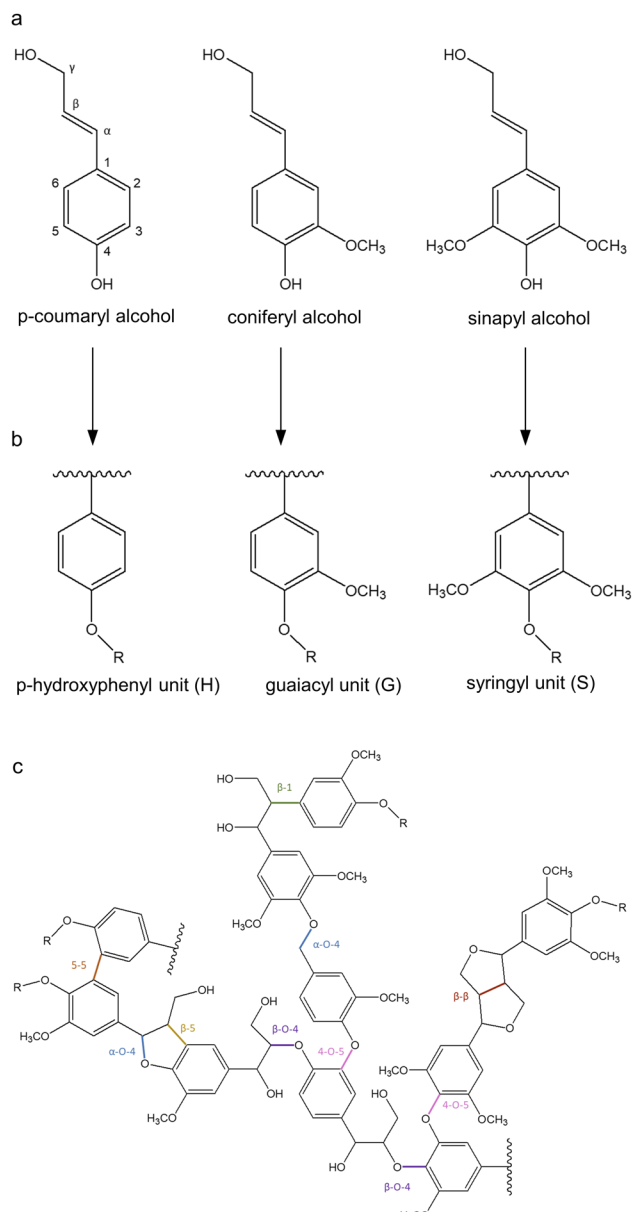


Fig. 2 Representation of (a) the main monolignols, (b) their units in lignin, and (c) lignin structure. Adapted from ref. 37 and 40.

The structure of lignin has been studied through numerous techniques, including nuclear magnetic resonance (NMR) spectroscopy, Fourier-transform infrared (FTIR) spectroscopy, Raman spectroscopy, and X-ray photoelectron spectroscopy.<sup>33,34</sup> It is generally accepted that lignin is a three-dimensional, highly branched, amorphous molecule composed of three basic phenylpropanoid units: *p*-hydroxyphenyl (H), guaiacyl (G), and syringyl (S) (Fig. 2b).

The biosynthetic pathway of lignin stems from the radical polymerization of three main monolignols, namely *p*-coumaryl alcohol, coniferyl alcohol, and sinapyl alcohol (Fig. 2a), which are derived from phenylalanine and differ in their degree of methylation. When monolignols are oxidized by laccase or peroxidase, they form radicals which undergo coupling reactions to form dilignols through C-C and C-O linkages, such as

$\beta$ -O-4,  $\beta$ -5, and  $\beta$ - $\beta$  bonds (Fig. 2c).<sup>35,36</sup> The biosynthesis of lignin results in heterogeneous interactions with S, G, and H units, whose content differs as a function of the plant species. For instance, in softwood lignins (from gymnosperms), G units are predominant, whereas hardwood lignins (from angiosperms) comprise equal amounts of G and S units, and herbaceous lignins are constituted by all three units, with H being less abundant.<sup>37</sup> The most stable bonds are 5-5 and  $\beta$ -5, which occur mainly between G units since S units have more methoxylated groups that block the C-5 position of the aromatic ring. Therefore, the lignin found in gymnosperms is more recalcitrant to chemical and microbial degradation, while angiosperm lignin is more likely to be less branched which can improve its processibility.<sup>38,39</sup>

### 2.3. Technical lignins and extraction methods

Lignins extracted from biomass feedstock after chemical processing are called technical lignins. The main industrial lignin extraction methods, originated from pulp and paper processes, are kraft pulping, soda pulping, and sulfite pulping, which yield kraft, soda, and lignosulfonate lignin, respectively.<sup>41,42</sup> The kraft method consists of alkaline hydrolysis with sodium hydroxide and sodium sulfide at high temperatures (150–170 °C), which cleaves the bonds between lignin and cellulose, and dissolves lignin. The product resulting from this process is hydrophobic lignin containing 1–3% sulfur in the form of aliphatic thiol groups, besides other functional groups including methoxy (14%), aliphatic (10%) and phenolic (2–5%) hydroxyl, and carboxylic acid (4–7%).<sup>5,43</sup> The sulfite process involves reactions between sulfur dioxide and sulfite salts in aqueous media at 125–150 °C and acidic pH. The lignin produced by this procedure is hydrophilic due to its high content of sulfonate groups (up to 13%).<sup>44</sup> The soda process uses alkaline hydrolysis with sodium hydroxide at high temperatures (140–170 °C) in the absence of sulfur-containing molecules, yielding hydrophobic lignin. These pulping methods are widely established in industry and produce highly pure lignin at elevated yields. However, due to the multiple chemical reactions occurring during these extraction processes, the structure of technical lignins differs significantly from that of native lignin. Partial biopolymer degradation also occurs during lignin extraction, thus decreasing its molecular weight. Moreover, harsh pH and temperature conditions are required, and toxic effluents are generated.

Other processes that are on the way of being established in industry are organosolv, acid hydrolysis, steam explosion, enzymatic hydrolysis, and ammonia fiber expansion pretreatments. Organosolv is another sulfur-free method that uses organic solvents such as ethanol in combination with acids and bases. This method allows the recovery of organic solvents, while highly pure, sulfur-free lignin is obtained. The native lignin structure with  $\beta$ -O-4 linkages is partially preserved after the treatment.<sup>45</sup> Recently, emerging processes using deep eutectic solvent (DES)<sup>46–48</sup> and biomass-derived organic solvents such as  $\gamma$ -valerolactone<sup>49,50</sup> have demonstrated potential for lignin isolation. These methods are able to preserve the lignin



structure (*i.e.*  $\beta$ -O-4 and  $\beta$ - $\beta$  linkages), while the solvents can be recovered and recycled,<sup>51,52</sup> thus moving toward a sustainable biorefinery concept by decreasing the amount of toxic solvents and pollutants. Selective enzymatic hydrolysis of biomass carbohydrates is used to purify lignin. Through this method, lignin is obtained in a quite high yield and its structure is considered to be chemically unaltered.<sup>53</sup> The main drawback of this method, however, is the presence of carbohydrate and protein impurities.

The properties of lignin such as molecular weight, functional groups, and solubility are important factors to be considered for the selection of a lignin type suitable for a desired application. Nevertheless, it is extremely difficult to correlate the lignin properties with the performance of the final material.<sup>27</sup>

#### 2.4. Bioactivities of lignin

Besides its structural role, native lignin also prevents the degradation of carbohydrates in plants by inhibiting the activity of bacteria and fungi. By analyzing plants with silenced genes participating in lignin biosynthesis, it has been demonstrated that the absence of lignin reduces resistance against bacterial and fungal pathogens.<sup>30</sup> Therefore, lignin is an important plant defense against microbial pathogens. The antimicrobial effect of the lignin structure has been associated with the presence of phenolic hydroxyl and methoxy groups.<sup>54</sup> When lignin is isolated from the plant, the extraction conditions can influence its antimicrobial potential due to the differences in molecular weight, functional groups, and solubility. For example, bacterial growth inhibition has been found in kraft lignin, while lignin extracted by simultaneous enzymatic saccharification and communication (SESC) has not shown such an inhibitory effect.<sup>14</sup> Other studies reported that lignin with isoeugenol structures possesses higher antibacterial activity than lignin with phenolic moieties containing oxygen ( $-\text{OH}$ ,  $-\text{CO}$ ,  $-\text{COOH}$ ) in the side chain.<sup>14</sup>

The mechanism of action of lignin against bacteria has not been completely elucidated. Some studies attribute the antibacterial activity of phenolic compounds to their ability to inhibit essential enzymes by generating hydrogen peroxide and complexing with metal ions,<sup>55</sup> in addition to their ability to destabilize bacterial membranes.<sup>56,57</sup> In the case of macromolecular lignin, it has been suggested that the phenolic hydroxyl groups promote a pH decrease around the cell, which destabilizes the membrane and eventually leads to the rupture of the cell.<sup>58</sup> These non-specific modes of action might reduce the possibility of resistance development in bacteria, thus contributing to overcoming antimicrobial resistance both in biomedical and phytosanitary applications.

Besides their antibacterial effect, the phenolic moieties of lignin also confer antioxidant and UV-blocking capacities. In an oxidative stress environment, phenolic structures can act as proton donors, converting free radicals into non-radical molecules. As a consequence, phenols are converted into phenoxy radicals that can react with another free radical to form a quinone.<sup>59</sup> For this reason, lignin can act as a scavenger preventing the adjacent molecules from oxidation. This

characteristic of lignin is of special interest in packaging to preserve the food properties, in dressing products for wound healing, and in cosmetic formulations for anti-aging.<sup>60</sup> On the other hand, the aromatic structures and carbonyl groups in lignin absorb visible and UV light (250–400 nm), acting as UV-blockers. Taking advantage of these properties, lignin has been tested as an active ingredient in sunscreen formulations.<sup>61,62</sup>

### 3. Lignin in antibacterial nanoformulations

Lignin has adopted different roles in the formulation of antibacterial NPs, including that of a main antibacterial agent, but also as a reducing agent, and as a carrier of other antibacterial agents.

#### 3.1. Lignin as an antibacterial agent in nanoformulations

In view of the potential of lignin as an antibacterial agent, several studies have reported LigNP dispersions capable of inhibiting bacteria (Table 1). There are different methods to synthesize these particles, among which solvent displacement, acid treatment, sonochemistry, and their combinations are the most common. Solvent displacement consists of mixing an organic solvent containing solubilized lignin with an excess of water, resulting in a gradual decrease of lignin solubility which rearranges into NPs.<sup>20</sup> Solvent displacement is a versatile technique that allows accurate control of the setting conditions, hence obtaining NPs with the desired characteristics. However, the low yield of NPs ( $\sim 1$  wt%) limits its application, especially on a large scale.<sup>19</sup> The acid precipitation method, developed by Frangville *et al.*, consisted of adding hydrochloric acid to a solution of lignin dissolved in ethylene glycol.<sup>63</sup> The method is based on initial lignin nucleation followed by particle growth from its molecular solution, which is promoted by the gradual addition of an aqueous solution of acid. In ultrasonication, LigNPs are formed by fractioning the large lignin macromolecule due to the cavitation phenomenon.<sup>64</sup> This process, however, induces the formation of radical oxygen species that can result in lignin oxidation. The morphology and size of LigNPs vary in function of the synthetic method and the experimental settings (Fig. 3a and Table 1). Spherical particles are commonly obtained from solvent displacement methods,<sup>65–67</sup> while acid treatment and ultrasonication yield irregular-shaped particles.<sup>64,68–70</sup>

Alkali lignin dissolved in ethylene glycol was subjected to different acidic conditions to prepare LigNPs (Fig. 3a(i)).<sup>70</sup> The particles presented different sizes ranging from 33 to 120 nm depending on the acid treatment with  $\text{HCl}$ ,  $\text{H}_2\text{SO}_4$ , or  $\text{H}_3\text{PO}_4$ . The antibacterial activity of the particles was assessed using three methodologies, namely spot diffusion assay, incorporation of lignin nanoparticles assay, and growth in broth assay. The results showed the capacity of the LigNPs to inhibit the growth and reduce the amount of viable plant pathogen Gram-negative bacteria (*Pseudomonas syringae* pv *tomato*, *Xanthomonas axonopodis* pv *vesicatoria*, and *X. arboricola* pv *pruni*).



Table 1 LigNPs in suspension used as antibacterial agents

Type of lignin	Particle preparation method	Particle shape	Particle size	Antibacterial activity	Ref.
Alkali	Acidolysis combined with sonochemistry	Irregular	33–120 <sup>a,c</sup> nm	<i>P. syringae</i> pv <i>tomato</i> , <i>X. axonopodis</i> pv <i>vesicatoria</i> , and <i>X. arboricola</i> pv <i>pruni</i>	70
Organosolv	Solvent displacement	Spherical	149–324 <sup>b,c</sup> nm	<i>E. coli</i> O157:H7 and <i>S. enterica</i> Typhimurium	65
Kraft	Solvent displacement combined with sonochemistry	Spherical	122.5 <sup>a</sup> nm	<i>E. coli</i> and <i>B. megaterium</i>	66
Alkali, aminated with ethylenediamine	Acidolysis combined with sonochemistry	Irregular	580 <sup>a</sup> nm	<i>S. aureus</i>	71
Soda	Sonochemistry	Irregular	217 <sup>b</sup> nm	<i>E. coli</i> , <i>S. aureus</i> , <i>P. aeruginosa</i> and <i>B. cereus</i>	69
Lignosulfonate (combined with chitosan)	Ultrasonication in oil/water	N.D.	221–234 <sup>a,c</sup> nm	<i>E. coli</i> , <i>S. aureus</i> and <i>B. subtilis</i>	72
Allyl-modified guaiacyl β-O-4 eugenol (lignin dimer)	Modification of MSNPs with a lignin dimer	Spherical	979 <sup>a</sup> nm	N.D.	67

<sup>a</sup> Obtained by dynamic light scattering. <sup>b</sup> Obtained by analyzing TEM images. <sup>c</sup> Depending on experimental conditions.

Therefore, the particles can be considered antibacterial agents for plant pathogen control.

Spherical LigNPs with different sizes were obtained by the solvent displacement approach, by dropping ethanol-solubilized organosolv lignin into water.<sup>65</sup> The NPs displayed

radical scavenging capacity and bacteriostatic effect at 1 mg mL<sup>-1</sup> against *Escherichia coli* O157:H7 and *Salmonella enterica* Typhimurium. Contrary to what was expected, the larger particles (324 nm) presented a higher inhibitory effect than the smaller ones (149 nm). Other physicochemical properties of the

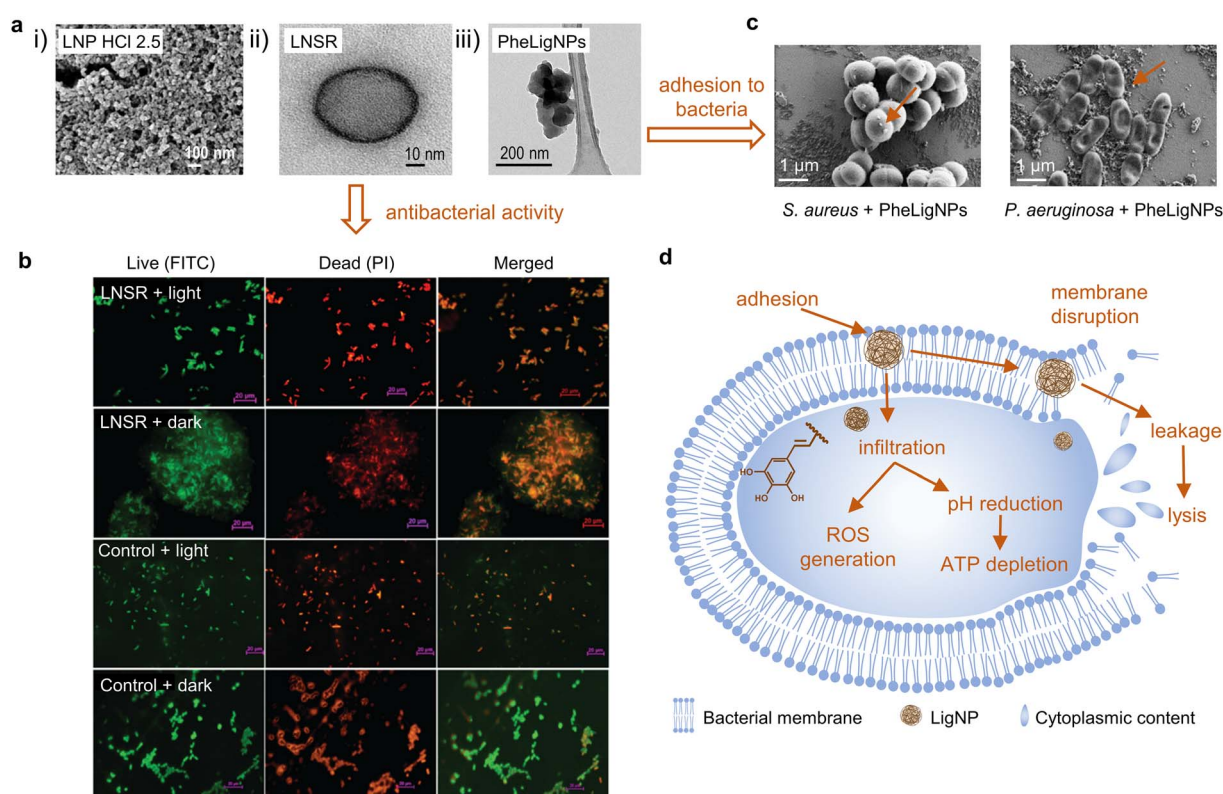


Fig. 3 (a) (i) FESEM image of clustered structured lignin nanoparticles after acidolysis (reproduced from ref. 70 with permission from American Chemical Society, copyright 2018), (ii) HRTEM image of the lignin nanospray (LNSR) (reproduced from ref. 66 with permission from the Royal Society of Chemistry), and (iii) HRTEM image of phenolated lignin nanoparticles (PheLigNPs) (reproduced from ref. 69 with permission from the American Society of Chemistry). (b) Fluorescence microscopy images of *E. coli* treated with the LNSR and untreated *E. coli* (control) in the light, stained with FITC and PI (at scale 20  $\mu$ m) (reproduced from ref. 66 with permission from the Royal Society of Chemistry). (c) SEM images of *S. aureus* and *P. aeruginosa* treated with subinhibitory concentrations of PheLigNPs (reproduced from ref. 69 with permission from the American Society of Chemistry). (d) Mechanisms for antibacterial behavior of extracted LNPs. Adapted from ref. 70.



particles, such as roughness, zeta-potential, and reactivity should be studied to explain the different antibacterial properties of these particles. The particles did not show cytotoxic effects on epithelial Caco-2 cells and also showed an antioxidant cellular effect by reducing the natural ROS level of the epithelial cells.

Paul *et al.* combined the solvent displacement method with sonochemistry to develop stable photodynamic lignin nanospheres in an aqueous medium to be used as lignin nanospray (LNSR) for microbial disinfection (Fig. 3a(ii)).<sup>66</sup> Under blue LED irradiation, the LNSR presented enhanced inhibition capacity toward Gram-negative *E. coli* and Gram-positive *Bacillus megaterium* compared to the LNSR under dark conditions (Fig. 3b). Studies on singlet oxygen generation revealed that the particles induced the formation of ROS under blue LED irradiation, which might explain the antibacterial activity of LNSR under this condition. The LNSR coated onto a glass slide prevented the growth of bacteria after blue LED exposure, which evidenced its suitability as a photodynamic coating material.

Lignin can be chemically modified in order to achieve superior antibacterial and antioxidant effects. Aminated LigNPs (a-LigNPs), prepared by acid precipitation followed by Mannich reaction surface modification, showed enhanced antioxidant activity in comparison with unmodified LigNPs.<sup>71</sup> However, the inhibition capacity toward *Staphylococcus aureus* was higher for LigNPs in comparison with a-LigNPs, which could be explained by the morphology of the particles: while LigNPs were quasi-spherical, a-LigNPs seemed glued together by a substance, and this might impede their penetration inside the cells. Given their improved UV-blocking capacity, a-LigNPs could find application in sunscreen lotions. In another study, lignin was enzymatically modified with tannic acid, a natural phenolic compound, to form NPs upon sonication (Fig. 3a(iii)).<sup>69</sup> The inhibitory capacity of phenolated lignin particles (PheLigNPs) against Gram-positive and Gram-negative bacteria was higher in comparison with that of bulk lignin, phenolated bulk lignin, and non-phenolated LigNPs. This demonstrated the contribution of both the nanosize and the phenolic content in the antibacterial activity of lignin. These results are in agreement with those of other studies reporting the inverse correlation between antibacterial activity and particle size.<sup>73–75</sup> PheLigNPs were able to adhere to the bacterial surface (Fig. 3c) and cause membrane disturbance, in addition to increasing the levels of ROS and reducing the metabolic activity of bacteria.

Lignin has also been combined with polymers or inorganic materials to enhance the antibacterial activity of nanoformulations. For instance, hybrid chitosan/lignosulfonate (CS-LS) NPs were prepared by sonochemistry taking advantage of the electrostatic interaction between the polymers.<sup>72</sup> The NPs inhibited the growth of Gram-negative *E. coli* and Gram-positive *S. aureus* and *Bacillus subtilis* at a higher rate than CS or LS alone. Moradipour *et al.* combined allyl-modified guaiacyl  $\beta$ -O-4 eugenol (G-eug), a lignin-derived dimer, with mesoporous silica NPs (MSNPs).<sup>67</sup> The particles were capable of interacting and disrupting synthetic lipid bilayers (representing bacterial model membranes), indicating their potential as antibacterial agents and drug carriers.

Several studies studied the effect of small phenolic compounds on bacteria.<sup>57,76,77</sup> However, very few studies analyzed the mechanism of action of macromolecular lignin or LigNPs. Despite being commonly accepted as antioxidants, phenolic compounds can exhibit pro-oxidant activity depending on their concentration and environmental factors.<sup>78</sup> In fact, it has been observed that polyphenols induce the generation of hydrogen peroxide, causing oxidative stress in bacterial cells.<sup>55</sup> Their antibacterial activity has also been related to their capacity to suppress the activity of essential enzymes.<sup>79,80</sup> Other studies have reported their capacity to weaken the bacterial membrane, increasing the permeability of the cell.<sup>56,57</sup>

In the case of LigNPs, it has been suggested that, due to their nanosize, LigNPs can penetrate the cell<sup>70</sup> where small phenolic compounds derived from lignin, such as cinnamaldehyde, would decrease the intracellular pH and cause ATP depletion.<sup>81</sup> This is in agreement with other studies reporting a decrease in metabolic activity of bacteria in the presence of subinhibitory concentrations of LigNPs.<sup>69</sup> Moreover, it has been demonstrated that LigNPs, due to their hydrophobic nature, can intercalate with the lipids of the bacterial envelope, causing a membrane disturbing effect.<sup>69</sup> The antibacterial mode of action of LigNPs also increases oxidative stress by inducing ROS generation.<sup>69,82</sup> Based on the reports summarized above, the mode of action of LigNPs would combine (1) penetration inside the cell resulting in increased levels of oxidative stress and decreased metabolic activity, and (2) adherence to bacterial cells and intercalation into the membrane, which eventually causes cell lysis (Fig. 3d).

### 3.2. Lignin as a reducing and capping agent of metal, metal oxide and metalloid nanoparticles

The combination of lignin with metal NPs has been extensively explored in the biomedical field, especially using lignin as a reducing agent (Fig. 4a and Table 2). Among antibacterial metals, silver has received special attention due to its ability to eradicate a broad range of microorganisms, and its ease of being reduced to form NPs. AgNPs exert their action against bacteria *via* different mechanisms, including (i) their attachment to the bacterial cell, increasing the permeability,<sup>83</sup> and (ii) the release of silver ions that penetrate into bacteria and produce free radicals.<sup>84,85</sup> The simultaneous action of AgNPs and their ions released leads to high levels of ROS, DNA damage, and cell death. Lignin-mediated synthesis of AgNPs is possible due to the phenolic hydroxyl groups of lignin, which are believed to interact with Ag<sup>+</sup> *via* cation–hydroxyl and cation– $\pi$  bonding and reduce them into metallic AgNPs.<sup>86,87</sup> In general, Ag<sup>+</sup> are more effective as antibacterial agents in comparison to AgNPs. However, once functionalized, AgNPs have shown superior antibacterial properties.<sup>88</sup> AgNPs can act as reservoirs of Ag<sup>+</sup> that are released in a sustained fashion, which is advantageous over free Ag<sup>+</sup> in terms of prolonged antibacterial action. This is especially beneficial in materials for biomedical applications requiring long-term antibacterial effects (e.g., implants and wound dressings). The presence of lignin as a capping agent of AgNPs confers several benefits on these antibacterial agents, including increased colloidal stability,



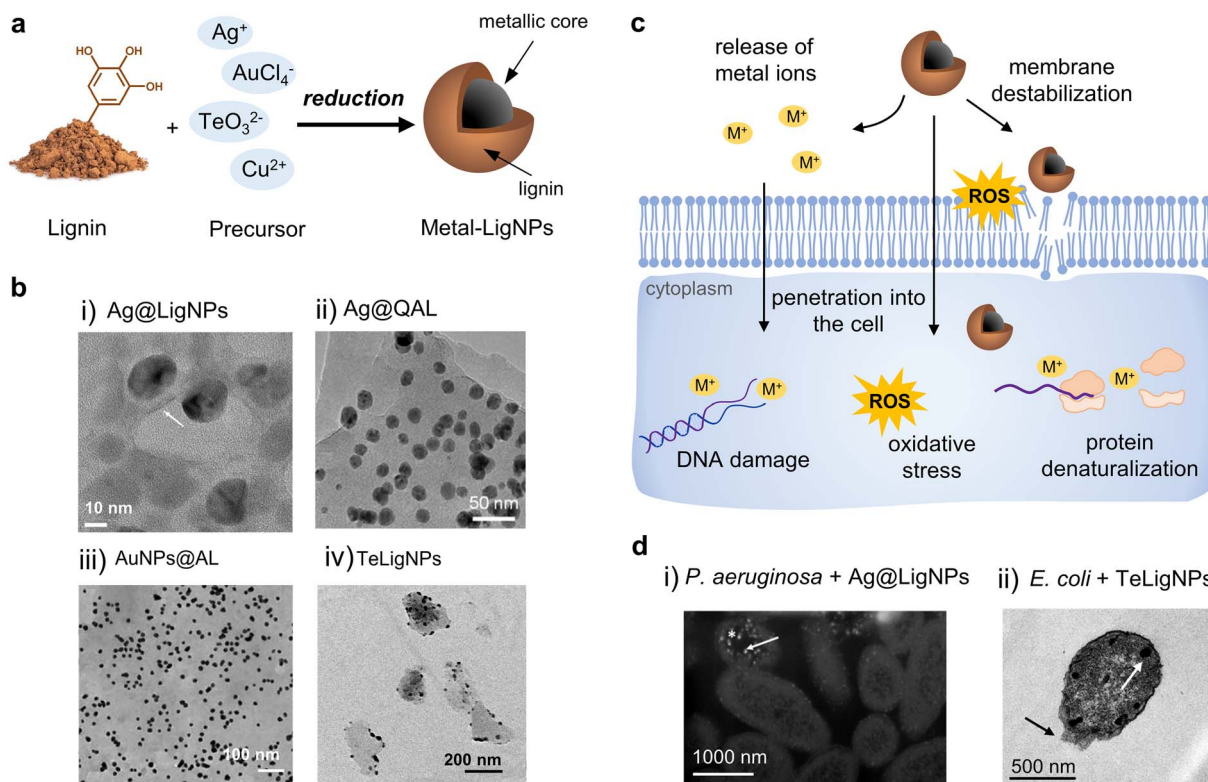


Fig. 4 (a) Schematic representation of the synthesis of metal-lignin NPs. (b) TEM images of (i)  $\text{Ag}@\text{LigNPs}$  (reproduced from ref. 89 with permission from the American Chemical Society) (ii)  $\text{Ag}@\text{QAL}$  (reproduced from ref. 98 with permission from Elsevier, copyright 2021), (iii)  $\text{AuNPs}@\text{AL}$  (reproduced from ref. 100 with permission from the Royal Society of Chemistry), and (iv)  $\text{TeLigNPs}$  (reproduced from ref. 101 with permission from the American Chemical Society). (c) Schematic representation of the antibacterial modes of action of metal-lignin NPs. (d) TEM images of (i)  $P. aeruginosa$  treated with  $\text{AgLigNPs}$  and (ii)  $E. coli$  treated with  $\text{TeLigNPs}$  (reproduced from ref. 89 and 101 with permission from the American Chemical Society).

Table 2 Lignin as a reducing and capping agent for the synthesis of hybrid antibacterial NPs

Type of lignin	Metal, metalloid or metal oxide	Particle shape <sup>a</sup>	Particle size <sup>a,b</sup>	Antibacterial activity	Ref.
Alkali	Ag	Spherical	~20 nm	<i>S. aureus</i> , <i>S. epidermidis</i> , <i>P. aeruginosa</i> , <i>K. pneumoniae</i> , <i>A. baumannii</i> , (MDR isolates and commercial strains), and <i>E. coli</i>	89
Alkali	Ag	Spherical	~20 nm	<i>Mycobacterium abscessus</i> in infected macrophages	90
Alkali	Ag	Spherical	~20 nm	<i>S. aureus</i> and <i>E. coli</i>	91 and 92
Kraft	Ag	Spherical	13 nm	<i>A. baumannii</i> , <i>P. aeruginosa</i> , <i>S. aureus</i> , <i>S. epidermidis</i> , <i>E. casseliflavus</i> , <i>K. pneumoniae</i> , and <i>A. baumannii</i> (MDR isolates)	93
Alkali	Ag	Spherical	10–50 nm	<i>S. aureus</i> , <i>E. coli</i> , and <i>A. niger</i>	94
N.D.	Ag	Quasi-spherical	50–80 <sup>c</sup> nm	<i>S. aureus</i> and <i>E. coli</i>	95
Organosolv	Ag	Spherical	10–50 nm	<i>S. aureus</i> , <i>B. circulans</i> , <i>P. aeruginosa</i> , <i>E. coli</i> , <i>B. subtilis</i> , and <i>R. eutropha</i>	96
Acid-alkaline	Ag	Spherical	15–25 nm	<i>E. coli</i>	97
Alkali, quaternized	Ag	Spherical	10–20 nm	<i>S. aureus</i> and <i>E. coli</i>	98
Alkali, quaternized	Ag	Spherical	25 nm	<i>S. aureus</i> and <i>E. coli</i>	99
Alkali, ZHL and alkali-extracted	Ag, Au	Spherical	8–25 <sup>c</sup> nm	<i>S. aureus</i> and <i>E. coli</i>	100
Soda	Te	Quasi-spherical	18 nm	<i>P. aeruginosa</i> and <i>E. coli</i>	101
Waste from the paper industry	$\text{Cu}_2\text{O}$	Quasi-spherical	100–200 nm	<i>S. aureus</i> and <i>E. coli</i>	102

<sup>a</sup> Refers to the metallic core. <sup>b</sup> Obtained by analyzing TEM images. <sup>c</sup> Depending on experimental conditions.

enhanced antibacterial activity, and reduced toxicity toward human cells.

In a recent study, alkali lignin served as a reducing and capping agent for the formulation of AgLigNPs by simply stirring the precursors for 3 days at 60 °C.<sup>89</sup> The resulting particles of ~20 nm (Fig. 4b(i)) were able to inhibit the growth of a broad range of bacterial strains, including multi-drug resistant (MDR) clinical isolates (*S. aureus*, *S. epidermidis*, *Pseudomonas aeruginosa*, *Klebsiella pneumoniae*, *Acinetobacter baumannii*, and *E. coli*), while a 5-fold higher amount of commercial AgNPs was needed for comparable efficacy. The increased antibacterial efficacy of the lignin-capped silver NPs was attributed to the ability of lignin to interact and disturb bacterial membranes, hence facilitating the penetration of Ag<sup>+</sup> ions inside the cell. Interestingly, such an interaction was only found with bacterial model membranes, while no effect was observed in mammalian model membranes.<sup>103</sup> This proves the contribution of lignin to the reduction of silver toxicity, as described in previous studies.<sup>104,105</sup> Following the above-described work, the authors incorporated the AgLigNPs into niosomes to target mycobacteria.<sup>90</sup> Niosomes are vesicles fabricated with a biomimetic cell membrane, which promotes their interaction with eukaryotic cells and the delivery of their cargo into the cytoplasm. *In vitro* assays against *Mycobacterium abscessus*, an intracellular pathogen causing lung infections, showed that it was resistant to the treatments with the NP-loaded niosomes, suggesting that the nanoniosomes did not merge with the bacterial cell wall. The antimicrobial effect was only observed in *M. abscessus*-infected macrophages, probably due to the fusion of the niosome with the eukaryotic cell membrane and the subsequent delivery of the bactericide cargo into macrophages.

Saratale *et al.* used alkali lignin extracted from wheat straw as a reducing, capping, and stabilizing agent for the synthesis of AgNPs by stirring for 60 min at 50 °C.<sup>91</sup> The lignin capping enhanced the free radical scavenging capacity of the AgLigNPs in comparison with the antioxidant capacity of AgNPs alone. The minimum inhibitory concentration (MIC) against *S. aureus* and *E. coli* was 25 and 20 µg mL<sup>-1</sup>, respectively. The combination of AgLigNPs with commercial antibiotics showed a synergistic antibacterial effect, suggesting the potential of this combination to combat MDR infections. Later, the authors studied the reusability of AgLigNPs in photocatalytic degradation, and also demonstrated their growth inhibition capacity against *S. aureus* and *E. coli*.<sup>92</sup> A different methodology for the kraft lignin-mediated synthesis of AgNPs was reported by Pletzer *et al.*, who described a fast microwave-assisted technique yielding lignin-capped AgNPs of 13 nm in diameter.<sup>93</sup> The NPs were tested against MDR clinical isolates. The highest antibacterial activity was found against Gram-negative *A. baumannii* and *P. aeruginosa*, with a MIC of ≤1.0 µg mL<sup>-1</sup>, while MICs of 2.5 and 5.0 µg mL<sup>-1</sup> were found for the other tested bacteria (*S. aureus*, *S. epidermidis*, *Enterococcus casseliflavus*, and *K. pneumoniae*). *In vitro* cytotoxicity studies with monocytic THP-1 leukemia cells demonstrated a lack of toxicity of these NPs at their antibacterial concentrations. In addition, *in vivo* studies using a skin abscess infection model in mice against MDR *P. aeruginosa* and methicillin-resistant *S. aureus* (MRSA) showed

a significant reduction in abscess sizes, while the Gram-negative bacteria load was reduced by 5-fold. The antibacterial effect of AgLigNPs demonstrated higher efficiency on Gram-negative bacteria than on Gram-positive bacteria. This tendency, which supports other AgLigNPs studies,<sup>89,95</sup> is attributed to the thicker peptidoglycan wall in Gram-positive bacteria which hinders the penetration of the NPs into the cell.

Marulasiddeshwara *et al.* used high molecular weight alkali lignin as a reducing and capping agent for AgLigNPs.<sup>94</sup> The resulting spherical shaped NPs, with an average size of 10–50 nm, were able to inhibit the growth of *S. aureus* and *E. coli*, and the fungi *Aspergillus niger*. Following the same procedure, Tran *et al.*<sup>95</sup> prepared AgNPs coated with rice-husk-extracted lignin or nano-lignin (LCSN and n-LCSP). It was found that lignin and nano-lignin were more antibacterial against Gram-positive *S. aureus* than against Gram-negative *E. coli*, while the (nano)-lignin-coated AgNPs presented a higher antibacterial effect against the Gram-negative bacterium.

Aadil *et al.* used lignin extracted from Acacia wood dust by the organosolv method to reduce silver and produce spherical AgNPs with a size of 10–50 nm.<sup>96</sup> The NPs displayed antibacterial properties against Gram-positive and negative strains, including the pathogens *S. aureus*, *Bacillus circulans*, *P. aeruginosa*, and *E. coli*. These NPs were also tested as colorimetric sensors for heavy metal ions, and as a redox catalyst, being able to reduce the methylene blue dye. Zevallos Torres *et al.* reported the acid–alkaline extraction of lignin from oil palm empty fruit bunches, which are by-products of the process of extracting edible and industrial oils, and its use as a reducing agent of silver ions.<sup>97</sup> After placing a solution of the extracted lignin in contact with a solution of AgNO<sub>3</sub>, spherical particles of 15–25 nm in diameter embedded in lignin were produced. The resulting NPs presented a MIC of 62.5 µg mL<sup>-1</sup> against *E. coli*, while the MIC of silver in ionic form was 31.25 µg mL<sup>-1</sup>. This difference was explained by the fact that AgNPs act as slow-release devices that prolong the antibacterial effect, while AgNO<sub>3</sub> in solution is already in the form of ions available to bacteria.

Microwave-assisted reduction of AgNO<sub>3</sub> by quaternized alkali lignin was reported by Wang *et al.*<sup>98</sup> The functionalization of lignin with the quaternary ammonium reagent (3-chloro-2-hydroxypropyltrimethylammonium chloride, CHMAC) provided positive charges that enhance the electrostatic interaction of the nanocomposite with negatively charged bacteria. The composites containing AgNPs and quaternized lignin (Ag@QAL) (Fig. 4b(ii)) were able to reduce viable *E. coli* by 3.72 log<sub>10</sub> (>99.9%) and *S. aureus* by 5.29 log<sub>10</sub> (>99.999%) CFU mL<sup>-1</sup>. The results indicated that quaternary ammonium lignin contributed to the antibacterial activity of the composites by enhancing the NP–bacteria interaction. The proposed antibacterial mechanism of action is based on the direct contact of Ag@QAL with the bacteria, induced by the positively charged quaternized lignin, followed by the generation of ROS by the nanosilver. Similarly, Li *et al.* prepared amphoteric lignin/nanosilver (AML@AgNPs) using lignin quaternized with CHMAC as a reducing and stabilizing agent.<sup>99</sup> Unmodified lignin presented a slight antibacterial effect against *S. aureus*,



while AML showed increased antibacterial properties that were attributed to the strong interactions between positively charged AML and negatively charged bacteria. The highest antibacterial capacity was observed for AML@AgNPs, which were able to completely eradicate *S. aureus* and *E. coli* at 60 and 30 ppm of Ag, respectively. Additionally, AML@AgNPs provided water-borne polyurethane (WPU) films with antibacterial properties. The authors demonstrated the adsorption of positively charged AML onto bacteria, which could enable the AgNPs to rapidly come into contact with bacterial cells and then exert their antibacterial effect.

Besides silver, lignin has also been used for reducing other metals, metalloids, and metal oxides to produce hybrid NPs. Rocca *et al.* provided a one-pot thermal and photochemical approach for the synthesis of lignin-doped silver and gold nanoparticles (Fig. 4b(iii)).<sup>100</sup> In general, all the tested lignins, namely low-sulfonate alkali lignin, ZHL lignin (depolymerized and 27% sugar content), and AL lignin (alkali-extracted, 16% sugar content), were able to reduce both metals and form spherical and monodispersed NPs. However, the antibacterial effect of the nanocomposites was clearly influenced by the nature of lignin, and only alkali and AL lignin produced antibacterial NPs. The AgNPs produced with alkali and AL lignin (AgNP@alkali and AgNPs@AL) exhibited antibacterial properties under light and dark conditions, with MIC values of  $0.2 \text{ }\mu\text{g mL}^{-1}$  and  $24.2 \text{ }\mu\text{g mL}^{-1}$ , respectively. In contrast, the lignin-coated AuNPs (AuNP@alkali and AuNPs@AL) only presented antibacterial activity under light irradiation and the MIC values were significantly higher ( $223\text{--}499 \text{ }\mu\text{g mL}^{-1}$ ). The AgNP@alkali and AgNPs@AL nanocomposites were able to completely eradicate *E. coli* and *S. aureus* within 30–40 min, while a longer time was required for the lignin-coated AuNPs (6 h). The results of ROS quantification in bacteria suggested that the mechanism of action of the NPs involved a photochemical process since elevated ROS values were detected after exposing the bacteria to the NPs under light conditions. Moreover, it was hypothesized that the sugars present in AL lignin might adhere to the peptidoglycan of the bacterial cell wall. Importantly, the particles were non-cytotoxic toward human cells at bactericidal concentrations. Preliminary assays show these AgNPs as potential antimicrobial agents towards *S. aureus* biofilm eradication.

In our group, lignin was used to develop hybrid tellurium-lignin nanoparticles (TeLigNPs) as alternative antimicrobial agents.<sup>101</sup> The sonochemically synthesized TeLigNPs are composed of a lignin matrix with embedded Te clusters, revealing the role of lignin as both a reducing agent and a structural component (Fig. 4b(iv)). The hybrid NPs showed strong bactericidal effects against Gram-negative *E. coli* and *P. aeruginosa*, achieving more than  $5 \log_{10}$  bacteria reduction. Exposure of TeLigNPs to human cells did not cause morphological changes or a reduction in cell viability. Studies on the antimicrobial mechanism of action demonstrated that the novel TeLigNPs disturb bacterial model membranes and generate ROS in Gram-negative bacteria. In another study, the lignin-mediated synthesis of crystalline  $\text{Cu}_2\text{O}$  NPs with a size of 100–200 nm was reported by Li *et al.*<sup>102</sup> Lignin derived from papermaking waste liquid reduced the Cu(II) ions from Cu(OH)<sub>2</sub>

to Cu(I) oxide NPs, and established a uniform coating on the surface of the particles. The NPs presented high antibacterial efficiency, being able to completely eradicate *E. coli* and *S. aureus* within 30 min.

Based on the experimental evidence from previous reports, the action of metal-lignin NPs against bacteria involves several mechanisms including (i) adhesion of AgNPs on the bacterial membrane causing structural damage, (ii) penetration into the cell and interaction with cytoplasmic biomolecules, (iii) generation of ROS and increasing the oxidative stress level of the cell, and (iv) interference with the signal transduction pathways by forcing the cell to intake extracellular signaling molecules (Fig. 4c and d).<sup>73,89,95,101</sup>

Typically, decreasing the particle size and increasing its roughness results in higher antibacterial activity because of the larger specific surface areas, which increases the probability of interacting with bacterial cells passing through their membrane.<sup>75,106,107</sup> However, other parameters such as the surface charge and the shape can also affect the antibacterial activity and should be also taken into account. Therefore, it is possible to control the physicochemical properties of NPs based on the final characteristics and activities of the particles, allowing their optimization for antibacterial applications.

### 3.3. Lignin nanocarriers

One of the emerging applications of lignin is its use as nanocarriers for biologically active substances, including antimicrobial agents, anti-cancer drugs, enzymes, and pesticides that should be delivered to a specific location under controlled conditions.<sup>23</sup> The advantage of using lignin as a nanocarrier is the increase in the stability of the loading substance, especially in the case of poorly water-soluble molecules. The most common approaches for loading bioactives in lignin carriers include entrapment (by infusion, solvent displacement, ion exchange, or coating), encapsulation by forming emulsions, and adsorption (Fig. 5). The loading of the active substance can take place during or after the formation of NPs. For instance, in the solvent displacement approach, the cargo is entrapped in lignin during the NP formation process. In the adsorption approach, the cargo is adsorbed onto previously synthesized LigNPs. The location of the cargo in the LigNP (*i.e.*, inside the particle or on its surface) may affect the functionality of the nanocarrier. For instance, encapsulation of the cargo inside the carrier may result in a slow release of the active substance and a prolonged antibacterial effect, while an active located on the surface is expected to have a burst release and shorter antibacterial effect. However, other factors such as cargo–NP interaction, hydrophobicity of the cargo, and covalent cross-linking should also be considered for predicting the behavior of the active substance. An overview of LigNPs used as carriers of different antibacterial agents can be found in Table 3.

Maldonado-Carmona *et al.* described the encapsulation of a porphyrin (5,10,15,20-tetrakis(4-hydroxyphenyl)-21H,23H-porphine, THPP) in acetylated lignin (AcLi) NPs by solvent displacement in dialysis membranes, achieving up to an 87.6% encapsulation rate.<sup>82</sup> Porphyrins are used as photosensitizers in



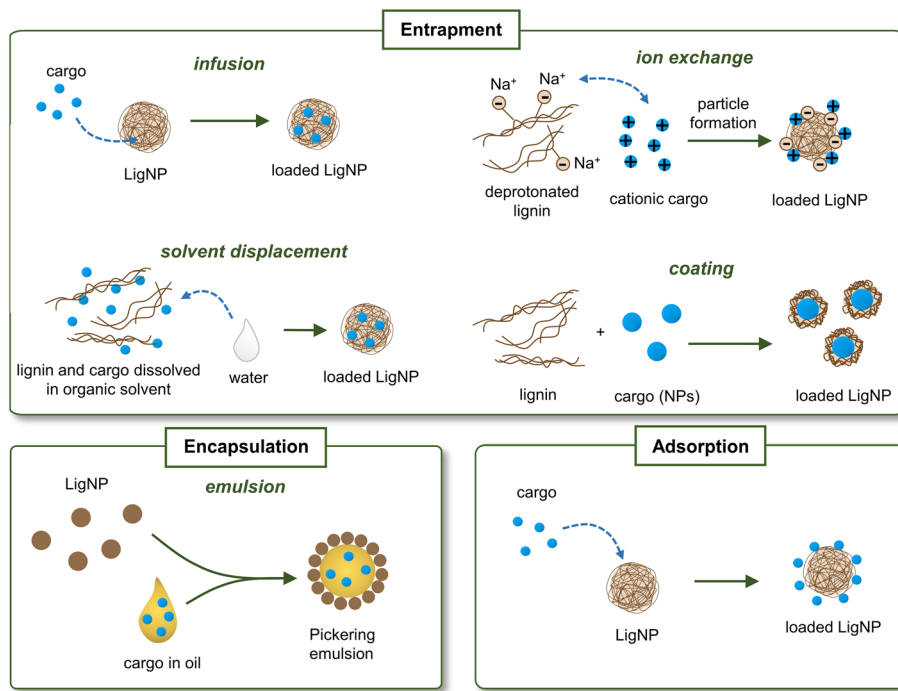


Fig. 5 Main strategies for loading actives into lignin nanocarriers.

antibacterial photodynamic therapy. Upon light irradiation, these molecules produce singlet oxygen which causes bacterial cell damage.<sup>119</sup> When exposed to light, THPP@AcLi was able to

drastically reduce the growth of Gram-positive bacteria (*S. aureus*, *S. epidermidis*, and *E. faecalis*) at low concentrations of porphyrin, while being ineffective against Gram-negative *E. coli*

Table 3 LigNPs as carriers of antibacterial agents

Type of lignin	NP preparation method	Loading strategy	Cargo	Particle shape	Particle size <sup>a</sup>	Antimicrobial activity	Ref.
Kraft, acetylated	Solvent displacement	Entrapment	Porphyrrins	Spherical	160–1348 <sup>b</sup> nm	<i>S. aureus</i> , <i>S. epidermidis</i> , and <i>E. faecalis</i>	82 and 108
Alkali Lignosulfonate, modified with an azo dye	Solvent displacement Chemical reduction to form ZnO	Emulsion Coating	Essential oils ZnO	Spherical Quasi-spherical	~200 nm 21–32 nm	<i>Penicillium italicum</i> <i>S. haemolyticus</i> , <i>C. diphtheriae</i> , <i>B. cereus</i> , <i>R. ornithinolytica</i> , <i>S. typhimurium</i> , <i>S. paratyphi</i> , <i>A. fumigatus</i> , <i>A. penicilloides</i> , <i>C. albicans</i> , <i>C. coronatus</i> , and <i>M. cookei</i>	109 110
Organosolv	Chemical reduction to form AgNPs	Adsorption	AgNPs	Quasi-spherical	28–54 <sup>b</sup> nm	<i>E. coli</i>	111
Lignosulfonate, PNMA-modified	Self-assembling, chemical reduction	Adsorption	AgNPs	Spherical	11 nm	<i>S. aureus</i> and <i>E. coli</i>	112
Kraft	Coating of lignin on silica followed by chemical reduction to form AgNPs	Adsorption	AgNPs	Irregular	30–36 nm	<i>B. subtilis</i> , <i>S. aureus</i> , <i>P. aeruginosa</i> , <i>E. coli</i> and <i>K. pneumoniae</i>	113
Kraft	Acid precipitation	Infusion	Ag <sup>+</sup>	Irregular	40–70 nm	<i>S. aureus</i> , <i>S. epidermidis</i> , <i>E. coli</i> , and <i>P. aeruginosa</i>	114
Kraft	Solvent displacement	Ion exchange	Ag <sup>+</sup>	Spherical	60–200 <sup>b</sup> nm	<i>S. aureus</i> , <i>E. coli</i> , and <i>P. aeruginosa</i>	115
Alkali Kraft Kraft	Emulsion evaporation Solvent displacement Emulsion and chemical reduction to form AgNPs	Entrapment Emulsion Adsorption	Enrofloxacin Ciprofloxacin AgNPs	Spherical Spherical Spherical	117 nm ~100 nm (DLS) 150 nm (SEM)	<i>E. coli</i> N.D. N.D.	116 117 118

<sup>a</sup> Obtained by analyzing TEM images. <sup>b</sup> Depending on setting conditions.

and *P. aeruginosa*. The researchers found that acetylated lignin NPs possess a bacteriostatic effect, and thus the antibacterial effect was attributed to the presence of porphyrin. It was shown that the NPs exerted their antibacterial action on the bacterial wall, without penetrating inside the cell. Given their antibacterial activity and light responsiveness, the porphyrin-loaded acetylated lignin NPs were proposed for photodynamic antimicrobial chemotherapy in wastewater purification. Later, in the same group, four different derivatives of THPP with different physicochemical characteristics (charge, size, and solubility) were encapsulated into AcLi.<sup>108</sup> The cationic porphyrins were able to reduce the growth of *E. coli* only in free form, but not after being encapsulated into AcLi NPs. Interestingly, for some porphyrins, the antibacterial efficacy against *S. aureus* increased in their encapsulated form in comparison with their free form.

Despite the potential of solvent displacement for the synthesis of lignin nanocarriers, volatile and flammable solvents such as tetrahydrofuran, acetone, and ethanol are typically used to produce these particles. These inherently hazardous chemicals might remain in the NPs, limiting their application in the biomedical field.<sup>120</sup> Alternative biomass-derived solvents are a greener option that would avoid safety issues. In these lines, Chen *et al.* synthesized LigNPs using a recycled  $\gamma$ -valerolactone (GVL)/water binary solvent (GWBS) system and two different nanoprecipitation methods – dropping and dialysis.<sup>109</sup> GVL is a non-toxic, non-volatile solvent obtained from cellulose feedstock that has been proposed as an alternative to toxic solvents in solvent displacement techniques. The resulting spherical lignin particles were used to prepare Pickering emulsions of essential oils, which are emulsions stabilized by surface active solid particles. The encapsulation of essential oils is expected to increase their stability, enhance their efficacy against microbes and hamper their volatilization. The antibacterial assay consisted of inoculating the fruit pathogen fungus *Penicillium italicum* in wounded oranges treated with essential oils dispersed in solvents or stabilized with LigNPs. The results showed that LigNPs promoted the growth inhibition activity of the essential oils towards the fungus.

Lignin has also been used to entrap previously synthesized metal oxide NPs. In a recent study, ZnO nanoparticles were entrapped by lignin modified with 2-[(E)-(2-hydroxy naphthalen-1-yl)diazenyl]benzoic acid, a photoactive azo dye, to obtain photoresponsive NPs for antimicrobial photodynamic therapy.<sup>110</sup> The antimicrobial activity assessed by the agar diffusion method showed that the hybrid particles after light irradiation presented high antibacterial activity against Gram-positive *Streptococcus haemolyticus*, *Corynebacterium diphtheriae*, and *Bacillus cereus*, presenting a zone of inhibition (ZOI) of 29–34 mm, and against Gram-negative *Raoultella ornithinolytica*, *Salmonella typhimurium*, and *Salmonella paratyphi* (ZOI ~ 26 mm). In addition, the particles were capable of inhibiting the growth of different fungal strains (*Aspergillus fumigatus*, *Aspergillus penicilloides*, *Candida albicans*, *Conidiobolus coronatus*, and *Microsporum cookei*), achieving a ZOI varying from 20 to 43 mm. In both antibacterial and antifungal tests, light irradiated

particles showed greater antimicrobial activity than non-irradiated particles.

Researchers have used LigNPs as carriers to entrap AgNPs as well. In these studies, lignin was not a reducing agent, but served as a carrier for AgNPs. For instance, Zhong *et al.* prepared lignin/AgNPs using citric acid or sodium borohydride as a reducing agent to obtain AgNPs that remained adsorbed onto the surface of organosolv lignin.<sup>111</sup> The nanocomposites were able to inhibit the growth of *E. coli* after 2 and 4 h of exposure. In another study, self-assembled poly(*N*-methylaniline)-lignosulfonate (PNMA-LS) composite microspheres with Ag<sup>+</sup> adsorbability were prepared.<sup>112</sup> After chelating Ag<sup>+</sup>, the reducing capacity of PNMA served to produce NPs of 11.2 nm that remained adsorbed onto the spheres. The PNMA-LS-Ag composite exhibited a strong bactericidal effect, with bactericidal rates of 99.95 and 99.99% for *E. coli* and *S. aureus* cells, respectively, which were higher than those obtained with free lignin and AgNPs. Another approach was used by Klapiszewski *et al.*<sup>113</sup> who combined kraft lignin with silica NPs as supports for AgNPs. The preparation route for composite NPs consisted of chemical reduction of Ag<sup>+</sup> by NaBH<sub>4</sub> followed by incorporation of the resulting AgNPs into previously hybridized and functionalized silica/lignin particles. Interestingly, increasing the amount of lignin in the hybrid materials resulted in higher adsorption rates of nanosilver onto their surface. The silica/lignin/AgNPs were able to inhibit the growth of *B. subtilis*, *S. aureus*, *P. aeruginosa*, *E. coli*, and *K. pneumoniae* achieving a ZOI of up to 12 mm for the highest concentration of NPs tested. The highest antibacterial effect was against *P. aeruginosa*, while *K. pneumoniae* was slightly inhibited by the particles. Correlation between Gram-staining and bacterial susceptibility to the antibacterial properties of the silica/lignin/AgNPs was not found in this work.

Despite the wide use of AgNPs as antibacterial agents in biomedical products,<sup>121</sup> their persistence in the environment coupled with their potential human health implications has raised some concerns.<sup>122,123</sup> Silver ions released from NPs were considered the main contributors to the cytotoxicity of AgNPs. However, studies show that Ag<sup>+</sup> released from AgNPs does not explain the toxicity effects caused by exposure to AgNO<sub>3</sub> at the same concentration.<sup>123</sup> Probably, the nanosize and specific properties of AgNPs also contribute to their cytotoxicity. The AgNP toxicity is both concentration and size-dependent, with high concentrations and smaller sizes being more toxic.<sup>124</sup> When it comes to Ag-containing NPs, it is thus important to tightly control the amount and the size of the NPs in order to avoid the cytotoxic effects of such NPs toward humans and the environment. Aiming to avoid the persistence of metal reservoirs after the intended use of such NPs, Richter *et al.* synthesized biodegradable Ag<sup>+</sup> infused NPs.<sup>114</sup> More specifically, nanoprecipitation of kraft lignin was used to prepare LigNPs which, in turn, were used as a core to infuse silver ions. Then, the resulting NPs were coated with a cationic electrolyte that increases their adhesion to the bacterial surface. In this work, instead of being the reducing agent of silver to produce AgNPs as described in the previous section, lignin was used as a nanocarrier of Ag<sup>+</sup>. The NPs, with sizes ranging from 40–



70 nm, presented high antibacterial activity against Gram-negative *E. coli* and *P. aeruginosa*, and Gram-positive *S. epidermidis* after a short time of exposure (1–30 min). The NPs

outperformed the AgNPs and Ag<sup>+</sup> solutions, even at lower Ag equivalents, suggesting an enhanced antibacterial effect due to the combination of Ag<sup>+</sup> and LigNPs. The silver-infused LigNPs

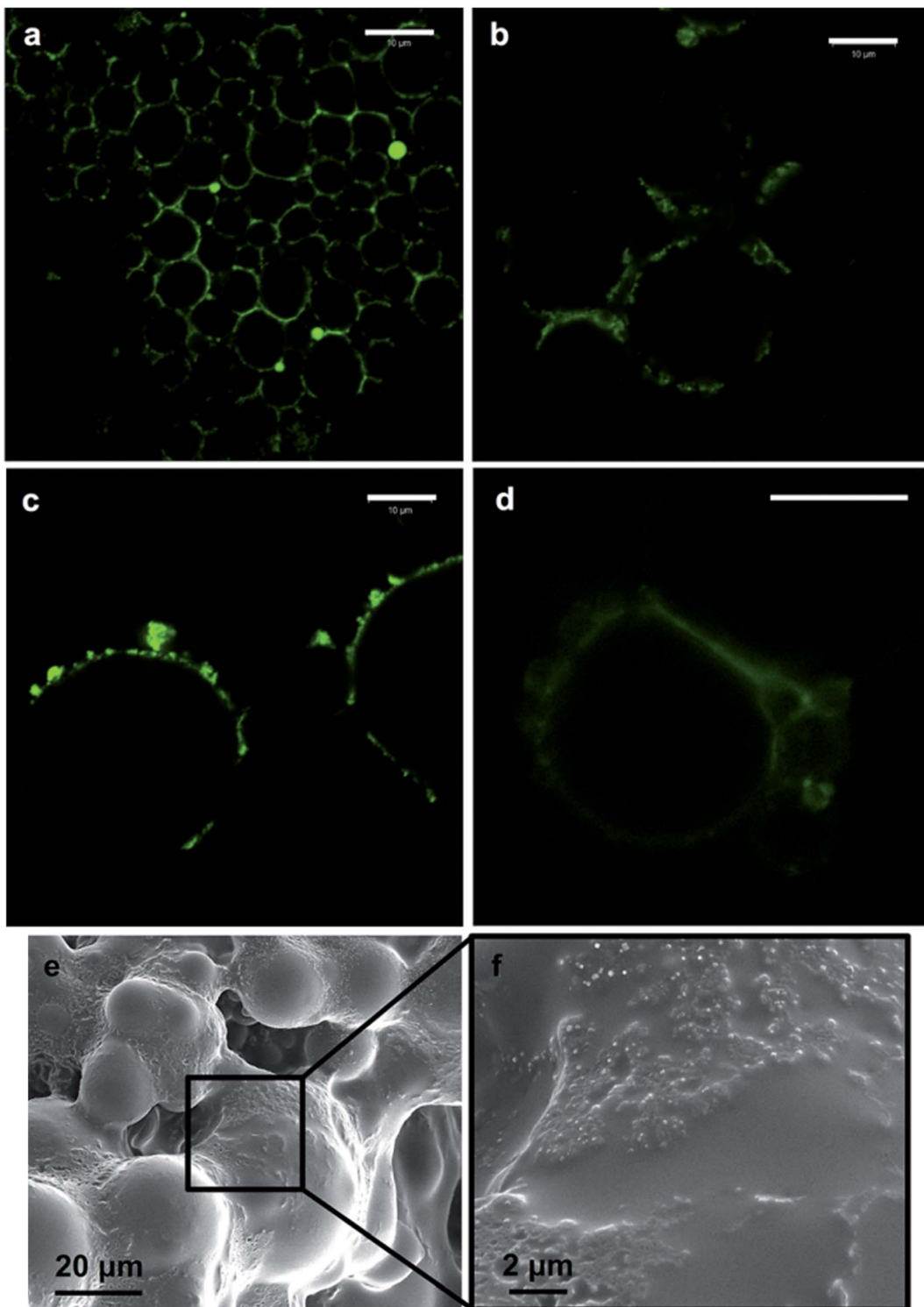


Fig. 6 Fluorescence imaging of hexadecane-in-water (oil volume fraction, 0.3) Pickering emulsions containing 0.6 (a) and 0.2 wt% (b) lignin particles (diameter, 320 nm). The case of emulsions with 0.2 wt% of lignin particles of larger (600 nm) (c) and smaller (90 nm) sizes (d) is also included. SEM images of lignin particles on a surface of an oil-in-water emulsion containing a photocured polymer (Norlan optical adhesive 81) as the oil phase and 0.4 wt% of the lignin particles in the aqueous phase are shown in (e) and (f), respectively. The scale bar in (a)–(d) is 10 μm. Reproduced from ref. 118 with permission from the Royal Society of Chemistry.



were dialyzed against water to simulate their depletion process, and only 18% of the total Ag remained in the particles after 24 h. It should be noted that the particles presented fewer cytotoxic effects than the free silver ions.<sup>105</sup> However, the fast release of Ag<sup>+</sup> from the lignin core reduces the shelf-life of these particles. Following a similar concept, Lintinen *et al.*<sup>115</sup> produced colloidal lignin particles (CLPs) where Ag<sup>+</sup> was ionically bound (AgCLPs). The synthetic procedure consisted of the deprotonation of kraft lignin, which led to sodium carboxylate and phenolate groups, followed by the binding of Ag<sup>+</sup> by ion exchange. Finally, the mixture of lignin with ionically bound Ag<sup>+</sup> was used to form NPs by solvent displacement. In this process, the recovered solvents can be reused for further synthesis cycles. Release of Ag<sup>+</sup> from the CLPs was not observed in water, but only under physiological conditions. The growth of *P. aeruginosa*, *E. coli* and *S. aureus* was inhibited by 94–96% in the presence of the AgCLPs. Interestingly, a synergistic effect of CLP and Ag<sup>+</sup> was observed for the Gram-positive bacteria.

Recently, Paudel *et al.* grafted lignin with poly(lactide-co-glycolide) (PLGA) for synthesizing nanocarriers by an emulsion evaporation method.<sup>116</sup> The particles were loaded with the poorly soluble antibiotic enrofloxacin for preventing the infection of *E. coli* O157:H7 in intestinal cells. The entrapment efficiency (EE) of the hybrid carriers (lignin-PLGA) was higher compared with that of PLGA carriers, probably because the hydrophobicity of the biopolymer increases the EE of LigNPs when it comes to low water-soluble drugs. The enrofloxacin-loaded nanocarriers were capable of inhibiting the growth of enteropathogenic *E. coli* by more than 50% at concentrations of 0.18 to 0.26 µg mL<sup>-1</sup>. The empty nanocarriers did not inhibit the growth of bacteria, hence the antibacterial effect was attributed to the presence of enrofloxacin. The enterocyte cell line IPEC-J2 showed over 70% viability in the presence of

nanocarriers at concentrations showing an antibacterial effect. An *in vitro* infection study using IPEC-J2 cells and *E. coli* showed that the nanodelivered enrofloxacin enhanced bacterial infection prevention in comparison with the free drug.

The broad interfacial compatibility of colloidal LigNPs allows their use as stabilizers in Pickering emulsions,<sup>125,126</sup> which are characterized by the presence of solid particles located at the oil–water interface that stabilizes the emulsion.<sup>127</sup> The surface activity of LigNPs, which is given by dissociation of phenolic groups under neutral to alkaline conditions, makes possible their use as stabilizers in these systems. Such emulsions can encapsulate lipophilic drugs for delivery purposes. In a study carried out by Zou *et al.*<sup>117</sup> nano-sized colloidal lignin particles (CLPs) with a layer of chitosan adsorbed on the surface (chi-CLPs) were used to prepare Pickering emulsions stabilizing ciprofloxacin-loaded olive oil. Ionic intra- and inter-particle crosslinking of the chitosan layer of the NPs was achieved using sodium triphosphate that further stabilized the droplets. The highest concentration of chi-CLP tested (1.0 wt%) resulted in emulsions with uniform oil droplets sized 10–20 µm, that were stable after more than 2 months. Ciprofloxacin showed a fast release at pH 2, 5.5, and 7.4, which was attributed to the small size of the droplets. Interestingly, the stability of the capsules was higher at acidic pH compared to pH 7.4, indicating their suitability for intestinal drug delivery. Nypelö and coworkers obtained spherical particles with tunable sizes from water-in-oil (W/O) microemulsions which are able to carry AgNPs.<sup>118</sup> The particles showed the capacity to stabilize hexadecane-in-water Pickering emulsions, forming oil droplets of 8 and 22 µm depending on the particle concentration (Fig. 6). The capacity of lignin-containing microemulsions to synthesize carriers of silver nanoparticles was demonstrated by mixing a microemulsion containing silver nitrate with another

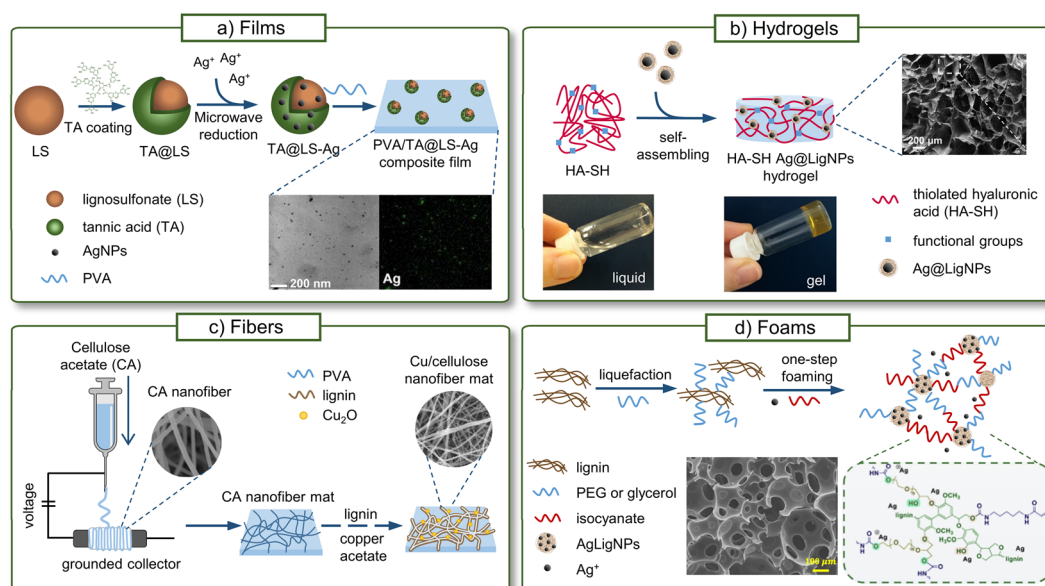


Fig. 7 Antibacterial materials containing LigNPs. (a) Films (adapted from ref. 132 with permission from John Wiley & Sons, copyright 2020), (b) fibers (adapted from ref. 137 with permission from Elsevier, copyright 2021), (c) hydrogels (adapted from ref. 130 with permission from the American Chemical Society) and (d) foams (adapted from ref. 134 with permission from the American Chemical Society, copyright 2022).



Table 4 Nanolignin-based film materials for food packaging applications

Type of lignin	Filler	Polymer matrix	Antimicrobial activity	Ref.
Extracted by steam explosion and enzymatic treatment	LigNPs	PVA, chitosan	<i>P. carotovorum</i> and <i>X. arboricola</i>	140
Steam explosion and enzymatic treatment	LigNPs, CNC	PLA	<i>P. syringae</i>	141
Alkali	aLigNPs, caLigNPs	PLA	<i>E. coli</i> and <i>M. luteus</i>	11
Soda	LigNPs	CNC, CNF	<i>S. aureus</i>	131
N.D.	LigNPs	CNF	<i>S. aureus</i> and <i>E. coli</i>	142
Alkali	LigNPs and metal oxide NPs	PLA	<i>S. aureus</i> and <i>E. coli</i>	143
N.D.	LigNPs and ZnO/Ag NPs	PLA	<i>S. aureus</i> and <i>E. coli</i>	144
Alkali	AgLigNPs	Cellulose	<i>E. coli</i>	145
Alkali	AgLigNPs	Agar	<i>L. monocytogenes</i> and <i>E. coli</i>	146
Organosolv	AgLigNPs	PLA	<i>L. monocytogenes</i> and <i>E. coli</i>	147
Lignosulfonate	TA@LS-Ag NPs	PVA	<i>S. aureus</i> and <i>E. coli</i>	132

containing sodium borohydride as the reducing agent. Even if the antimicrobial activity of these particles was not evaluated, we hypothesize that they could be efficient antibacterial agents due to the presence of AgNPs.

## 4. Antibacterial composite materials containing lignin nanoparticles

Due to their higher specific surface area, NPs are known to improve the stiffness, strength, toughness, thermal stability, and barrier properties of polymeric materials better than traditional fillers, even at low concentrations (1–5 wt%).<sup>128</sup> In recent years, LigNPs have been incorporated into a variety of composite materials not only for improving the mechanical properties of the material, but also to provide antibacterial, antioxidant, anticorrosion, and UV-blocking activities, and metal adsorbent capacity.<sup>129</sup>

In this section, the different antibacterial composite materials containing LigNPs, alone or in combination with other polymers or metals, will be reviewed. Such materials can be prepared by incorporating previously synthesized NPs,<sup>130–133</sup> or using an *in situ* approach where the NP synthesis takes place in the material.<sup>87,134–136</sup> Some of these materials include films, hydrogels, fibers, and foams, which have been validated as food packaging materials, wound dressings, medical coatings, or in other biomedical applications (Fig. 7).

### 4.1. Food packaging

The growth of microorganisms in food is a serious concern because it causes a reduction in the shelf-life of food and increases the risk of acquiring food-borne infections causing illness in almost 1 in 10 people in the world.<sup>138</sup> Hence, preventing the contamination of food to avoid food-borne infections is crucial. Ideal advanced materials for food packaging should be antimicrobial and antifouling agents to avoid the proliferation of bacteria and fungi, antioxidants to preserve the properties of food, and resistant to humidity. Moreover, biomass sources for environmentally friendly and biodegradable packaging are interesting since they can potentially substitute traditional petroleum-based plastics. Lignin, as a natural antioxidant and antibacterial polymer, is a suitable

filler for food packaging materials, especially in the form of NPs that additionally improve the mechanical performance of the material.<sup>139</sup> Table 4 gives an overview of the film materials in which LigNPs or their derivatives have been used as multifunctional fillers.

An example of these packaging materials is found in the work by Yang *et al.*, who incorporated LigNPs obtained by hydrochloric acidolysis into poly(vinyl alcohol) (PVA) and PVA/chitosan films produced by solvent casting.<sup>140</sup> The phenolic and aliphatic hydroxyl groups of LigNPs interacted with the hydroxyl groups of PVA and the amino groups of chitosan. The DPPH assay revealed that the nanocomposites presented a radical scavenging activity of 70.5–91.7%, with a clear dependence on the amount of LigNPs. The growth of plant pathogenic *Pectobacterium carotovorum* and *X. arboricola* was reduced in the presence of PVA/LigNP and PVA/chitosan/LigNP, while no growth inhibition was observed with the PVA and PVA/chitosan films without NPs. LigNPs not only conferred bioactivities to the films but also improved their mechanical performance, showing an increase in the tensile strength from 45.8 to 51.5 MPa in PVA/LigNP films. Moreover, the thermal analysis showed that the LigNPs enhanced the crystallization of PVA, probably acting as heterogeneous nucleating agents. The incorporation of LigNPs and cellulose nanocrystals (CNCs) into poly(lactic acid) (PLA) films was also explored by Yang and coworkers.<sup>141</sup> The combination of the two nanofillers in the polymeric film increased its crystallinity and tensile strength, and imparted UV light blocking capability. Only the films containing LigNPs were able to reduce the growth of the plant pathogen *Pseudomonas syringae*, indicating the role of LigNPs in the antibacterial activity. However, the binary PLA/LigNP film presented higher antibacterial activity than PLA/CNC/LigNP. The presence of CNCs clearly contributed to the high degree of crystallinity of the films, which may decrease the diffusion of LigNPs and their antibacterial response. Similarly, with the aim of improving the dispersibility of the fillers in PLA/LigNPs formulations, Cavallo *et al.* used acetylated LigNPs (aLNPs) and citric acid-treated LigNPs (caLNPs) as nanofillers in PLA films.<sup>11</sup> The incorporation of acetyl in aLNPs, and ester and ether in caLNPs had a significant effect on their compatibility with the PLA matrix, and the aggregation of the modified fillers at 1 wt% in PLA films decreased in comparison with that in



pristine LigNPs. However, self-aggregation was observed in increasing concentrations of fillers regardless of the chemical modification. The growth of *E. coli* and *Micrococcus luteus* was reduced after incubation with PLA films containing LigNPs, aLNPs, and caLNPs. However, the antibacterial effect was more pronounced in the case of Gram-positive *M. luteus*. The aLNPs significantly increased the antibacterial activity of the composites, whereas their antioxidant and UV blocking capacities were not improved with the chemical modification of lignin.

In a recent study, the effect of the polymerization degree and the functional groups of lignin on the properties of films based on CNCs and cellulose nanofibrils (CNFs) was studied.<sup>131</sup> The two forms of lignin, *i.e.* phenol-enriched oligomer fractions and colloidal LigNPs, showed different effects on the antioxidant activity of cellulose films. Lignin oligomers enhanced the radical scavenging capacity, while LigNPs reduced it, probably as a consequence of the less accessible phenolic groups in the colloidal particles. In contrast, the antibacterial properties were not affected by the molecular weight: all the formulations reduced the growth of *S. aureus* by 0.3–0.5 log. However, the growth of *E. coli* was not affected. In view of the properties of cellulose and lignin films, both LigNPs and lignin oligomers can be potentially used as active additives in food packaging. In another study, LigNPs obtained from corncob lignin *via* the anti-solvent precipitation method were blended with CNFs to prepare biodegradable films.<sup>142</sup> The presence of LigNPs increased the hydrophobicity of the films and provided UV and visible light blocking capacities, which are desirable features in food packaging. However, the tensile stress and elongation of CNF-based composite films decreased after the addition of LigNPs. The hybrid films reduced the growth of *S. aureus* and *E. coli* in comparison to the CNF films.

Lizundia *et al.* showed the benefits of the incorporation of metallic NPs into transparent PLA films to be used in the packaging industry.<sup>148</sup> Later, the authors introduced LigNPs and inorganic metal oxide NPs into these films.<sup>143</sup> The combination of metal oxides and LigNPs provided high UV-protection capacity and antioxidant activity, with superior results obtained only with inorganic NPs. Another study combining metal/metal oxide NPs (ZnO/Ag) with LigNPs in PLA composites was carried out by Deng *et al.*, obtaining nanocomposites with multiple functionalities.<sup>144</sup> To overcome the common dispersion issues in the PLA matrix, polypyrrole glutinous nanofibrils crosslinked with dopamine (PPy-PDa) were used as particle dispersants. The films containing LigNPs did not produce a ZOI on agar plates where *E. coli* and *S. aureus* were grown. However, after adding hybridized PyDa-ZnO/Ag, a ZOI of both bacteria was observed. Therefore, ZnO/Ag was responsible for the antibacterial properties of the films, while LigNPs increased the thermal stability and improved the mechanical properties of the composites.

As mentioned in the previous sections, one of the most efficient methods for controlling the growth of microorganisms is the use of AgNPs. However, concerns about the safety of human health and the environment appear related to the diffusion of such NPs into food, and thus, the release of AgNPs

from food packaging materials should be rigorously controlled. According to the European Food Safety Authority (EFSA), using AgNP additives at low concentrations (up to 0.025% w/w) in polymers that do not swell should not raise safety concerns for the consumer, since under these conditions the release of silver is below the acceptable daily intake.<sup>149</sup>

Lignin-capped AgNPs were prepared on the surface of cellulose fibrous membranes, achieving a load of AgNPs of about 3%.<sup>145</sup> The characteristic plasmon resonance peak of AgNPs in the UV-vis spectra was observed for the composites. However, the peak did not appear in the rinsing water after sonication of the composites. This suggested that the AgNPs were strongly anchored to the cellulose fibers, probably through hydrogen bonding, and were not released into the aqueous medium. The composite showed strong bactericidal activity, achieving complete eradication of *E. coli* after 10 min of contact in suspension. Growth inhibition was also observed on the agar plate (ZOI 8–10 mm), suggesting some release of silver ions. The presence of lignin on the cellulose materials conferred UV-blocking capacities in both UV-B and UV-C regions and also improved their thermal stability. This work demonstrated the multiple functionalities of lignin incorporated into the hybrid AgNPs, including complexing and reducing properties for Ag<sup>+</sup> and binding of the NPs to the cellulose material. The absence of Ag release makes this material suitable for food packaging applications.

Alkali lignin was used as a reducing and capping agent for the synthesis of AgLigNPs that were incorporated into agar and glycerol to form films.<sup>146</sup> The agar films containing lignin in bulk form did not show antibacterial activity, while the films containing AgLigNPs were capable of eradicating the food-borne pathogens *L. monocytogenes* and *E. coli* within 9–12 h. The highest antibacterial efficiency was observed against *E. coli*, which was attributed to the thinner peptidoglycan layer of the Gram-negative bacteria. In addition to the bactericidal properties, the AgLigNPs also increased the tensile strength, water vapor barrier, and UV-light barrier properties. In a later work, the authors used organosolv lignin to prepare AgLigNPs as additives for antibacterial PLA composite films.<sup>147</sup> However, the AgLigNPs were poorly dispersed in the polymer matrix and formed aggregates when higher concentrations of particles were used (1 wt%). The nanocomposites showed high antibacterial capacity and were able to fully eradicate *L. monocytogenes* and *E. coli* within 6 and 3 h, respectively. Similar to their previous work, the incorporation of AgLigNPs provided a UV screening effect and antibacterial properties and improved the mechanical, water vapor barrier, and thermal stability properties of the PLA films. Zhang *et al.* prepared TA@LS-Ag NPs using tannic acid as a reducing agent and lignosulfonate as a carrier and dispersing agent (Fig. 7a).<sup>132</sup> By comparing the different hybrid NPs (TA-Ag, LS-Ag, TA@LS, and TA@LS-Ag), the authors demonstrated the important role of lignin in the antibacterial activity of the particles, since it significantly reduced the minimum inhibitory and bactericidal concentrations of TA@LS-Ag in comparison with TA-Ag. The ternary particles provided PVA films with antibacterial activity, being able to inhibit the growth of *S. aureus* and *E. coli*. TA@LS-Ag also



Table 5 Nanolignin-embedded antibacterial polymeric materials for biomedical applications

Type of lignin	Filler	Polymer matrix	Material	Antimicrobial activity	Application	Ref.
Extracted by steam explosion and enzymatic treatment	LigNPs	PVA and chitosan	Hydrogel	<i>S. aureus</i> and <i>E. coli</i>	Biomedical, generic	153
Lignosulfonate	PANI-LIG: $\text{Fe}_3\text{O}_4$ @GS	N.A.	Coating onto titanium	<i>S. aureus</i> , <i>E. coli</i> , and <i>C. albicans</i>	Coating for medical implants	154
Alkali	AgLigNPs	CA, AA, and P(AAm-co-AA)	Hydrogel fibers	<i>E. coli</i>	Coating for PPE	155
N.D.	AgLigNPs	PU and ionic liquids	Ionogel	<i>S. aureus</i> and <i>E. coli</i>	Sensor	156
Alkali	AgLigNPs	PEGDGE	Hydrogel	N.D.	Sensor	157
Lignocellulosic biomass	AgLigNPs	Lignocellulose	Hydrogel	<i>E. coli</i>	Wound healing	87
Alkali	AgLigNPs	Pectin and PAA	Hydrogel	<i>S. aureus</i> and <i>E. coli</i>	Wound healing	158
Alkali	AgLigNPs	HA-SH	Hydrogel	<i>S. aureus</i> and <i>P. aeruginosa</i>	Wound healing	130
Alkali	AgLigNPs	PAHC	Hydrogel	<i>E. coli</i> , <i>S. aureus</i> , MRSA, and <i>C. albicans</i>	Wound healing	159
Alkali	AgLigNPs	Carageenan	Hydrogel	<i>S. aureus</i> and <i>E. coli</i>	Wound healing	86
Alkali	LNP-Ag and CNCs	PVA	Hydrogel	<i>S. aureus</i> and <i>E. coli</i>	Wound healing	160
Kraft	Ag/Au NPs	PAA	Hydrogel	<i>C. albicans</i>	Wound healing	161
Lignosulfonate	AgNPs	Aminated lignin and PVA	Hydrogel	<i>S. aureus</i> and <i>E. coli</i>	Wound healing	162
Organosolv	AgNPs	Lignin and PVA	Nanofiber mats	<i>E. coli</i> and <i>B. circulans</i>	Wound healing	163
Alkali	AgLigNPs	PAN	Nanofibers	<i>S. aureus</i> and <i>E. coli</i>	Wound healing	164
Alkali	CuO	CNF	Nanofibers	<i>S. aureus</i> and <i>E. coli</i>	Wound healing	137
Soda	AgPheLigNPs	PU	Foam	<i>S. aureus</i> and <i>P. aeruginosa</i>	Wound healing	133
Extracted by enzymolysis	AgLigNPs	PU	Foam	<i>S. aureus</i> and <i>E. coli</i>	Wound healing	134

improved the mechanical performance of the films, showing very high toughness and tensile strength values, which were attributed to the dense hydrogen bonding interactions between the particles and the PVA matrix.

#### 4.2. Biomedical applications

The interest in utilizing lignin as a functional additive for biomedical applications has increased over the past years, demonstrating the suitability of lignin for the development of advanced and sustainable biomaterials. LigNPs have been studied as vehicles for drug and gene delivery, as biosensors, for tissue engineering, *etc.*<sup>150,151</sup> This section focuses on antibacterial biomedical materials containing LigNPs, comprising hydrogels, films, nanofibers, and foams (Table 5). Long-lasting antibacterial properties of these materials are required, which are usually achieved by a sustained release of the active NPs over time. However, such release of NPs together with the degradation products of the polymeric matrix may cause cell inflammation.<sup>152</sup> Thus, an in-depth investigation of the cytotoxicity and biocompatibility of these materials should be conducted before their application to human health.

A facile approach for the development of antibacterial nanolignin-based materials is to use LigNPs as fillers in a polymeric matrix. For instance, hydrogels of PVA and chitosan embedding LigNPs as antibacterial fillers were prepared by Puglia *et al.*<sup>153</sup> The resulting PVA/Ch/LigNPs gels were able to reduce the number of viable *E. coli* and *S. aureus* by 2 log.

Bacterial reduction was also observed in the PVA/Ch gels prepared without NPs, especially against *E. coli*, probably due to the presence of antibacterial chitosan. On the other hand, the growth of planktonic *S. epidermidis* was only reduced by the hydrogels containing LigNPs, even though the reduction was modest (~0.3 log). However, the gels were not efficient against *S. epidermidis* biofilms, which reflects the much higher resistance of biofilm-forming bacteria to antibacterial agents.

For some biomedical applications, such as implantable medical devices and their packaging, an environment completely free from bacteria is required. To this end, the medical devices should possess a strong antibacterial effect that prevents the colonization of bacteria and biofilm formation. The combination of biocompatible LigNPs with strong antibacterial metals is a common approach for achieving such performance.

**4.2.1. Coatings.** Bacterial adhesion on biomedical devices and subsequent biofilm formation is a major concern from health and economic perspectives. An approach to prevent bacterial contamination and proliferation is surface coating with antibacterial NPs. An example of an antibacterial coating for implantable titanium devices is found in the work of Visan *et al.*, who developed nanostructured coatings based on polyaniline grafted lignin (PANI-LIG) embedded with magnetite nanoparticles loaded with aminoglycoside gentamicin sulfate (GS) ( $\text{Fe}_3\text{O}_4$ @GS).<sup>154</sup> The coatings were anticorrosive, antioxidant, and more hydrophilic than the bare titanium surface. The formation of *E. coli*, *S. aureus*, and *C. albicans* biofilms on the coatings was inhibited by ~3, ~1.5, and ~1.5 log, respectively,



in 24 h. On the other hand, human osteoblast-like cells did not lose viability when grown onto the surface of the PANI-LIG:Fe<sub>3</sub>O<sub>4</sub>@GS coatings, which makes the application of these materials as medical implants feasible. In another study, highly stretchable hydrogel fibers based on AgLigNPs, citric acid (CA), acrylic acid (AA), and poly(acrylamide-co-acrylic acid) (P(AAm-co-AA)) were prepared by He *et al.*<sup>155</sup> The AgLigNPs, obtained by lignin-mediated reduction, participated in the gelation process by initializing the radical polymerization of monomers and, owing to the quinone-catechol reversible reactions, provided the hydrogel with adhesion properties. CA was added to the formulation to create reversible bonds that improve the deformability and stretchability of the gel, enabling its manufacturing in the form of fibers with a diameter of 50  $\mu\text{m}$ . The hydrogels demonstrated antibacterial activity against *E. coli*, achieving a 1.8 log reduction after 24 h. When the hydrogel fibers were coated onto a mask (*i.e.* personal protective equipment) by electrospinning, a 100% eradication of *E. coli* was achieved.

**4.2.2. Sensors.** Skin-like wearable sensors are medical devices used for personal health monitoring (*e.g.*, glucose, uric acid, and lactose) that can be fabricated as hydrogels, films and membranes.<sup>165</sup> Hydrogel sensors with multifunctional properties have gained attention due to their hydration, biocompatibility, and ionic sensor capabilities. An ideal skin sensor should feature good mechanical properties, long-lasting adhesion, and antibacterial properties. A skin wearable ionogel sensor based on modified polyurethane (PU) and ionic liquids, containing AgLigNPs as active fillers, was developed by Wang *et al.*<sup>156</sup> The gel was characterized by high elongation and tensile strength and, owing to the thiol groups present in the modified polyurethane, a self-healing ability. The catechol chemistry of AgLigNPs provided adhesiveness to the material, as well as contact killing capacity toward *E. coli* and *S. aureus*. In addition, the compatibility of ionic liquids with polymers conferred electrical conductivity.

In another study, AgLigNPs were used as crosslinking points for preparing poly(ethylene glycol) diglycidyl ether (PEG-DGE) hydrogels with pressure sensing properties.<sup>157</sup> Besides providing adhesion and pH-responsiveness, the AgLigNPs are also expected to confer a strong antibacterial capacity on the hydrogels.

**4.2.3. Wound healing.** The development of mechanically stable and biocompatible wound dressings capable of maintaining a local bacteria-free and moist environment, is crucial for the successful healing of wounds. Wounds, and in particular those that do not heal within several weeks (chronic wounds) are characterized by highly inflammatory conditions, a large number of pathogenic bacteria, biofilms, an excess of free radicals, and dysregulation of hydrolytic enzymes that degrade the extracellular matrix. Efficient dressing materials could be engineered by incorporating active NPs with multiple functionalities including antioxidant, antimicrobial, enzyme inhibition, and anti-inflammatory properties that promote wound healing into the dressings. In the design of materials for wound treatment, lignin is frequently found in combination with metals to enhance the antibacterial activity of the dressing to

achieve efficient pathogen elimination (Table 5). Different nanolignin-based materials for wound healing have been developed, mainly hydrogels, nanofibers, and polyurethane foams.

**Hydrogels.** Hydrogels are polymeric networks capable of absorbing and retaining large amounts of liquids, *e.g.* wound exudates, and are considered optimal materials for wound healing due to their flexibility, capacity to maintain a moist environment favorable for healing, and biodegradability. Advanced hydrogel dressings should incorporate multifunctional agents to ensure antibacterial and antioxidant capacities.<sup>166</sup> In the case of hybrid silver/lignin NPs as actives in hydrogels for wound treatment, examples of their use can be found in Gan *et al.* where novel pectin and poly(acrylic acid) (PAA) hydrogel was built using AgLigNPs as antibacterial and crosslinking agents.<sup>158</sup> Ammonium persulfate (APS) produced free radicals in lignin, which initiated the polymerization of the hydrogel. The hydrogels presented bactericidal properties *in vitro*, being able to reduce cultures of *S. aureus* and *E. coli* by 98 and 97%, respectively, and *in vivo* in a rabbit model. The catechol-based chemistry was mainly responsible for the durable adhesiveness of the gels. The *in vitro* studies showed the capacity of the gels to promote cell adhesion and proliferation, while the *in vivo* tests with rats validated the wound healing and skin tissue regeneration capacities of the hydrogel.

Our group developed a self-assembling injectable hydrogel based on modified thiolated hyaluronic acid (HA-SH) and Ag@LigNPs (Fig. 7b).<sup>130</sup> The lignin-capped NPs were responsible for the gelation through multiple polymer–NP interactions, comprising hydrogen bonding, thiol–π, and cation–π. These dynamic non-covalent interactions imparted self-healing and injectability to these materials. The hydrogels displayed strong bactericidal activity, achieving a 7 and 4.5 log reduction of *P. aeruginosa* and *S. aureus*, respectively, while cytotoxicity toward human keratinocytes was not observed. Interestingly, the release of silver was sustained over time (following zero-order kinetics), which is expected to prolong the antibacterial activity and reduce possible side effects. *In vivo* studies in mice showed a rapid closure of the wound after the treatment with the gel, complete regeneration of the skin and a lack of signs of inflammation or bacterial infection. Similarly, using an *in situ* synthetic approach, AgNPs obtained by lignin-mediated reduction were used as crosslinking agents to construct hydrogels based on phenylboronic acid-modified hydroxypropyl cellulose (PAHC).<sup>159</sup> The dynamic borate ester bonds of catechol groups of lignin with the phenylboronic acid groups in PAHC provided self-healing and shape adaptive properties. Moreover, the hydrogels were capable of adhering to different tissues and inorganic materials through hydrogen bonding, and electrostatic and ion coordination interactions. The gels presented radical scavenging ability and completely eradicated *E. coli*, *S. aureus*, the yeast *C. albicans*, and MRSA. *In vivo* studies with a MRSA-infected wound model showed that the hydrogels accelerated the epithelial tissue regeneration, reduced the inflammatory cell infiltration, and significantly promoted wound healing. The *in situ* reduction of silver into hydrogels was also achieved using the lignin from lignocellulosic biomass as



a reducing and capping agent.<sup>87</sup> By adjusting the content of lignin in the hydrogel, AgLigNPs of different sizes were obtained (10–40 nm). The hydrogels inhibited the growth of *E. coli*, obtaining a larger ZOI with the increase of lignin content in the material.

The one-pot synthesis of carrageenan-based AgLigNP-enabled hydrogels was performed by Jaiswal *et al.* using lignin as a reducing and capping agent, and divalent cations (CaCl<sub>2</sub>, CuCl<sub>2</sub>, and MgCl<sub>2</sub>) as crosslinking agents.<sup>86</sup> The presence of AgLigNPs increased the tensile strength and elongation of the hydrogel while completely eradicating *E. coli* and *S. aureus* within 3–6 h. The hydrogels showed good biocompatibility with dermal fibroblasts *in vitro* and were capable of improving the healing of wounds in rats. Yang *et al.* studied the effect of silver/lignin NPs and CNCs in PVA hydrogels.<sup>160</sup> The hydrogels were prepared by first embedding AgNPs onto the surface of LigNPs by a direct reduction of silver nitrate, and then PVA was cross-linked with glutaraldehyde in the presence of CNCs and Ag loaded LigNPs (LNP–Ag). The addition of the nanofillers allowed the pore structure and mechanical properties of the material to be tuned. The hydrogels containing LigNPs presented a slight antibacterial effect against *S. aureus* and *E. coli*, tested by the agar diffusion method, which was significantly improved when LNP–Ag was added. The gels containing LigNPs and LNP–Ag exhibited radical scavenging activity unlike the PVA and PVA/CNC hydrogels alone. The wound healing and skin regeneration tested *in vivo* in mice were accelerated by the Ag-containing hydrogel, which was attributed to the gradual release of LNP–Ag from these hydrogels.

An *in situ* approach for the synthesis of AgNPs into a lignin-based hydrogel was chosen by Li *et al.*<sup>162</sup> First, lignosulfonate was aminated through the Mannich reaction and was then crosslinked with PVA to form a hydrogel. Afterwards, silver nitrate was added and AgNPs were formed by reduction within the hydrogel. The hydrogel completely eradicated *E. coli* and *S. aureus* within 6 and 9 h, respectively, and reduced the cell viability of mouse fibroblast cells (L929 cell line) by 25%.

The use of hybrid lignin-bimetallic NPs in hydrogels for wound healing has been explored by Chandna *et al.*<sup>161</sup> using Kraft lignin as a reducing and stabilizing agent for the synthesis of Ag/Au NPs conjugated with the photosensitizer rose bengal and doped into a PAA hydrogel. A rapid release of the nanoactives occurred at acidic pH due to degradation of the hydrogel under this condition. After excitation with a green laser, the number of viable yeast (*C. albicans*) decreased. These results demonstrated the applicability of the hydrogels in antimicrobial photodynamic therapies for infected acute wounds, where the environment is mostly acidic.

**Nanofibers.** AgNPs were synthesized *in situ* onto the surface of polyacrylonitrile (PAN) nanofibers using lignin as a reducing agent.<sup>164</sup> The presence of lignin not only provided antioxidant capacities but also significantly promoted the NPs' anchoring onto the nanofibers. The antibacterial activity of the PAN/AgNPs composites tested by the agar diffusion method showed a ZOI of ~13–21 mm against *S. aureus* and *E. coli*, achieving higher values by increasing the concentration of the silver precursor. In contrast, PAN nanofibers without NPs did not inhibit the

growth of bacteria. The antibacterial activity of the nanocomposites was attributed to the burst release of silver within the first 2 h, followed by a sustained release over several days. These nanofibrous materials were considered suitable for the treatment of acute wounds.

The *in situ* lignin-mediated synthesis of CuO nanoparticles on the surface of electrospun CNF as potential wound dressings was also explored by Haider *et al.* (Fig. 7c).<sup>137</sup> CuO/CNF released 80% of the copper ions within the first 24 h, reaching a plateau in the release during the next 5 days. The growth of *S. aureus* and *E. coli* was inhibited by CuO/CNF (ZOI 1.9–2.8), while the viability of a NIH3T3 fibroblast cell line was over 80% after 7 days of incubation in the presence of the nanofibers. Moreover, the presence of lignin conferred antioxidant properties on the nanofibers. The incorporation of AgNPs into lignin/PVA nanofibrils was carried out by Aadil *et al.*<sup>163</sup> In this work, lignin was not in the form of NPs but as a polymer matrix together with PVA in the electrospun nanofibers. The material was capable of inhibiting the growth of *E. coli* and *B. circulans* in the agar diffusion test, showing a larger ZOI than antibiotic discs.

**Polyurethane foams (PUFs).** Flexible PUFs have the capacity to absorb large amounts of wound exudates and can be easily adapted to different wound shapes. In our group, silver/phenolated lignin NPs (AgPheLigNPs) were incorporated into flexible PUFs to generate multifunctional wound dressings.<sup>133</sup> First, lignin was enzymatically modified with tannic acid, a natural phenolic compound, to increase its reactivity. Then, the phenolated lignin was used to reduce Ag<sup>+</sup> in an ultrasonic field and produce AgPheLigNPs that were blended with the PU precursors prior to polymerization in order to incorporate them permanently into the PUF structure. The nanocomposite foams showed strong antibacterial activity, achieving a 4.6 and 5.6 log reduction against *S. aureus* and *P. aeruginosa*, respectively. The foams released less than 1% of Ag in a sustained manner, indicating that the majority of Ag remained immobilized in the PUF. Additionally, the swelling capacity, density, and compression modulus of the resulting PUFs can be tuned by varying the amount of AgPheLigNPs.

A different approach for the synthesis of lignin-based PUFs (LPUFs) was adopted by Li *et al.*,<sup>134</sup> where AgNPs were formed *in situ* by lignin-mediated reduction (Fig. 7d). The synthetic procedure of these composite foams comprised liquefaction of lignin with poly(ethylene glycol) and glycerol, followed by simultaneous foaming and AgNP formation. The swelling behavior of the resulting AgNP-LPUFs was influenced by the presence of hydrophobic lignin and AgNPs by decreasing the water uptake ability of the foams. The AgNP-LPUFs gradually reduced the number of viable *S. aureus* and *E. coli* over time, achieving a reduction of above 99% after 8 h. However, the antibacterial activity of the foams against *S. aureus* was significantly lower than that against *E. coli*. The LPUF without AgNPs also present some antibacterial activity against *E. coli*, which was attributed to the intrinsic antibacterial activity of lignin. *In vivo* studies in mouse wound models showed that the group treated with AgNP–PUF exhibited better wound area closure than those treated with PUF, LPUF, and a commercial dressing without antibacterial agents.



## 5. Final remarks

Nanoformulation of lignin in antibacterial materials is an emerging valorization approach for this underutilized biopolymer. Extensive research on antibacterial LigNPs and their combination with metals, antibiotics, and polymers has been conducted in the last few years. Particular attention has been placed on lignin-mediated synthesis of AgNPs and their incorporation into materials as multifunctional agents. The fact of using lignin as a largely available biomass material for the synthesis of antibacterial NPs reduces the environmental impact of these materials. However, a broader analysis of the sustainability of the process, from the lignin extraction method to the formulation of the final material, should be performed. In any case, the use of toxic solvents, chemical crosslinkers, or chemical reducing agents should be avoided to minimize both the human toxicity and environmental hazard risks.

An extensive study of the antibacterial properties of LigNPs, preferably through standardized methods, would benefit the research community when it comes to assessing the potential applications of NPs. For instance, strong bactericidal activity is required for advanced wound dressing materials, while a bacteriostatic effect is enough for avoiding the growth of pathogens in food packaging. On the other hand, the antibacterial mode of action of lignin and LigNPs needs to be elucidated. Studies on the penetration capacities of LigNPs inside bacterial cells, as well as their membrane-disturbing capacities, would be useful to understand the different efficacies against Gram-positive and negative bacteria. Acquiring comprehensive knowledge of how LigNPs inhibit the growth of microorganisms is crucial for developing effective antimicrobial composites for a broad range of applications.

In order to bring nanolignin-based materials to the market, their synthetic procedures should be simplified and upscaled, while maintaining low manufacturing costs. Overcoming the problem of lignins' intrinsic heterogeneity is a critical issue for obtaining reproducible materials. Despite studies showing the advantages of highly antibacterial lignin materials for food and biomedical applications, safety data and clinical experience are required before their commercialization. Although lignin has been approved as a food additive by some regulatory bodies, its use in the form of NPs as a food contact substance (e.g., in food packaging) has not been regulated so far. In the case of lignin-based materials for wound healing, their classification in the proper medical device class is primordial for performing the appropriate clinical evaluation.<sup>167</sup> Nevertheless, there is still a lack of specific regulatory guidance over nanomaterials in general and lignin-based materials, in particular, for biomedicine, which may hinder their entry into the market.<sup>168,169</sup> It is thus important to focus future research on the physicochemical characteristics of nanoscale materials and understand their interactions with biological systems, which is crucial for their approval by the regulatory bodies. In this review, we highlighted the versatility of antibacterial LigNPs in terms of synthetic procedures, their multiple functionalities due to the nanoformulation, and their compatibility with a variety of materials,

demonstrating the enormous potential of these natural antibacterial agents.

## Conflicts of interest

There are no conflicts of interest to declare.

## Acknowledgements

This work received funding from the European Research Council (ERC) under the European Union's Horizon 2020 Research and Innovation Program (Biomat Project, H2020-NMBP-TO-IND-2018-2020, Grant Agreement Number 953270). A. G. Morena acknowledges Agència de Gestió d'Ajuts Universitaris i de Recerca (Generalitat de Catalunya) for providing her the PhD grant (2019FI\_B 01004).

## References

- 1 B. Hu, K. Wang, L. Wu, S. H. Yu, M. Antonietti and M. M. Titirici, *Adv. Mater.*, 2010, **22**, 813–828.
- 2 J. Vanneste, T. Ennaert, A. Vanhulsel and B. Sels, *ChemSusChem*, 2017, **10**, 14–31.
- 3 A. J. Ragauskas, G. T. Beckham, M. J. Biddy, R. Chandra, F. Chen, M. F. Davis, B. H. Davison, R. A. Dixon, P. Gilna, M. Keller, P. Langan, A. K. Naskar, J. N. Saddler, T. J. Tschaplinski, G. A. Tuskan and C. E. Wyman, *Science*, 2014, **344**, 1246843.
- 4 G. Koch, in *Handbook of Pulp*, John Wiley & Sons, Ltd, 2008, vol. 1, pp. 21–68.
- 5 N. E. El Mansouri and J. Salvadó, *Ind. Crops Prod.*, 2006, **24**, 8–16.
- 6 B. M. Upton and A. M. Kasko, *Chem. Rev.*, 2016, **116**, 2275–2306.
- 7 A. Grossman and V. Wilfred, *Curr. Opin. Biotechnol.*, 2019, **56**, 112–120.
- 8 Z. Zhang, V. Terrasson and E. Guénin, *Nanomaterials*, 2021, **11**, 1336.
- 9 B. Del Saz-Orozco, M. Oliet, M. V Alonso, E. Rojo and F. Rodríguez, *Compos. Sci. Technol.*, 2012, **72**, 667–674.
- 10 P. K. Mishra and R. Wimmer, *Ultrason. Sonochem.*, 2017, **35**, 45–50.
- 11 E. Cavallo, X. He, F. Luzi, F. Dominici, P. Cerrutti, C. Bernal, M. L. Foresti, L. Torre and D. Puglia, *Molecules*, 2020, **26**, 126.
- 12 M. Tortora, F. Cavalieri, P. Mosesso, F. Ciaffardini, F. Melone and C. Crestini, *Biomacromolecules*, 2014, **15**, 1634–1643.
- 13 F. Shu, B. Jiang, Y. Yuan, M. Li, W. Wu, Y. Jin and H. Xiao, *Biomacromolecules*, 2021, **22**, 4905–4918.
- 14 B. Ndaba, A. Roopnarain, M. O. Daramola and R. Adeleke, *Sustainable Chem. Pharm.*, 2020, **18**, 100342.
- 15 S. Sugiarto, Y. Leow, C. L. Tan, G. Wang and D. Kai, *Bioact. Mater.*, 2022, **8**, 71–94.
- 16 P. Duarah, D. Haldar and M. K. Purkait, *Int. J. Biol. Macromol.*, 2020, **163**, 1828.



17 Q. Tang, Y. Qian, D. Yang, X. Qiu, Y. Qin and M. Zhou, *Polymers*, 2020, **12**, 1–22.

18 M. H. Hussin, J. N. Appaturi, N. E. Poh, N. H. A. Latif, N. Brosse, I. Ziegler-Devin, H. Vahabi, F. A. Syamani, W. Fatriasari, N. N. Solihat, A. Karimah, A. H. Iswanto, S. H. Sekeri and M. N. M. Ibrahim, *Int. J. Biol. Macromol.*, 2022, **200**, 303–326.

19 S. Beisl, A. Miltner and A. Friedl, *Int. J. Mol. Sci.*, 2017, **18**, 1244.

20 S. Iravani and R. S. Varma, *Green Chem.*, 2020, **22**, 612–636.

21 P. K. Mishra and A. Ekielski, *Nanomaterials*, 2019, **9**, 243.

22 W. D. H. Schneider, A. J. P. Dillon and M. Camassola, *Biotechnol. Adv.*, 2021, **47**, 107685.

23 M. H. Sipponen, H. Lange, C. Crestini, A. Henn and M. Österberg, *ChemSusChem*, 2019, **12**, 2039.

24 K. Chen, S. Wang, Y. Qi, H. Guo, Y. Guo and H. Li, *ChemSusChem*, 2021, **14**, 1284.

25 D. Piccinino, E. Capecci, E. Tomaino, S. Gabellone, V. Gigli, D. Avitabile and R. Saladino, *Antioxidants*, 2021, **10**, 274.

26 S. Beisl, A. Friedl and A. Miltner, *Int. J. Mol. Sci.*, 2017, **18**, 2367.

27 E. Lizundia, M. H. Sipponen, L. G. Greca, M. Balakshin, B. L. Tardy, O. J. Rojas and D. Puglia, *Green Chem.*, 2021, **23**, 6698–6760.

28 J. Barros, H. Serk, I. Granlund and E. Pesquet, *Ann. Bot.*, 2015, **115**, 1053–1074.

29 F. J. Ruiz-Deñas and Á. T. Martínez, *Microb. Biotechnol.*, 2009, **2**, 164–177.

30 M. Lee, H. S. Jeon, S. H. Kim, J. H. Chung, D. Roppolo, H.-J. Lee, H. J. Cho, Y. Tobimatsu, J. Ralph and O. K. Park, *EMBO J.*, 2019, **38**, e101948.

31 F. G. Calvo-Flores, J. A. Dobado, J. Isac-García and F. J. Martín-Martínez, in *Lignin and Lignans as Renewable Raw Materials*, John Wiley & Sons, Ltd, 2015, pp. 9–48.

32 E. Capanema, M. Balakshin, R. Katahira, H. M. Chang and H. Jameel, *J. Wood Chem. Technol.*, 2014, **35**, 17–26.

33 N. M. Stark, D. J. Yelle and U. P. Agarwal, in *Lignin in Polymer Composites*, Elsevier Inc., 2016, pp. 49–66.

34 Y. C. Y. Lu, Y. C. Y. Lu, H. Q. Hu, F. J. Xie, X. Y. Wei and X. Fan, *J. Spectrosc.*, 2017, **2017**, 1–15.

35 W. Boerjan, J. Ralph and M. Baucher, *Annu. Rev. Plant Biol.*, 2003, **54**, 519–546.

36 R. Katahira, T. J. Elder and G. T. Beckham, *RSC Energy Environ. Ser.*, 2018, **2018**, 1–20.

37 S. Laurichesse and L. Avérous, *Prog. Polym. Sci.*, 2014, **39**, 1266–1290.

38 R. Vanholme, B. Demedts, K. Morreel, J. Ralph and W. Boerjan, *Plant Physiol.*, 2010, **153**, 895–905.

39 E. M. Anderson, M. L. Stone, R. Katahira, M. Reed, W. Muchero, K. J. Ramirez, G. T. Beckham and Y. Román-Leshkov, *Nat. Commun.*, 2019, **10**, 2033.

40 F. G. Calvo-Flores and J. A. Dobado, *ChemSusChem*, 2010, **3**, 1227–1235.

41 H. Lange, S. Decina and C. Crestini, *Eur. Polym. J.*, 2013, **49**, 1151–1173.

42 H. Chung and N. R. Washburn, in *Lignin in Polymer Composites*, Elsevier Inc., 2016, pp. 13–25.

43 C. Crestini, H. Lange, M. Sette and D. S. Argyropoulos, *Green Chem.*, 2017, **19**, 4104–4121.

44 T. Aro and P. Fatehi, *ChemSusChem*, 2017, **10**, 1861–1877.

45 D. R. Lobato-Peralta, E. Duque-Brito, H. I. Villafán-Vidales, A. Longoria, P. J. Sebastian, A. K. Cuentas-Gallegos, C. A. Arancibia-Bulnes and P. U. Okoye, *J. Cleaner Prod.*, 2021, **293**, 126123.

46 C. Fernandes, E. Melro, S. Magalhães, L. Alves, R. Craveiro, A. Filipe, A. J. M. Valente, G. Martins, F. E. Antunes, A. Romano and B. Medronho, *Int. J. Biol. Macromol.*, 2021, **177**, 294–305.

47 E. O. Owhe, N. Kumar and J. G. Lynam, *Biocatal. Agric. Biotechnol.*, 2021, **32**, 1878–8181.

48 Z. Chen, A. Ragauskas and C. Wan, *Ind. Crops Prod.*, 2020, **147**, 112241.

49 M. A. Ahmed, J. H. Lee, A. A. Raja and J. W. Choi, *Appl. Sci.*, 2020, **10**, 1599.

50 S. Jampa, A. Puente-Urbina, Z. Ma, S. Wongkasemjit, J. S. Luterbacher and J. A. Van Bokhoven, *ACS Sustainable Chem. Eng.*, 2019, **7**, 4058–4068.

51 X. J. Shen, J. L. Wen, Q. Q. Mei, X. Chen, D. Sun, T. Q. Yuan and R. C. Sun, *Green Chem.*, 2019, **21**, 275–283.

52 H. Q. Lê, J. P. Pokki, M. Borrega, P. Uusi-Kyyyny, V. Alopaeus and H. Sixta, *Ind. Eng. Chem. Res.*, 2018, **57**, 15147–15158.

53 K. Radotić and M. Mićić, in *Sample Preparation Techniques for Soil, Plant, and Animal Samples*, Humana Press, New York, NY, 2016, pp. 365–376.

54 G. Wang, Y. Xia, B. Liang, W. Sui and C. Si, *J. Chem. Technol. Biotechnol.*, 2018, **93**, 2977–2987.

55 H. Arakawa, M. Maeda, S. Okubo and T. Shimamura, *Biol. Pharm. Bull.*, 2004, **27**, 277–281.

56 T. P. T. Cushnie and A. J. Lamb, *Int. J. Antimicrob. Agents*, 2011, **38**, 99–107.

57 L. Bouarab-Chibane, V. Forquet, P. Lantéri, Y. Clément, L. Léonard-Akkari, N. Oulahal, P. Degraeve and C. Bordes, *Front. Microbiol.*, 2019, **10**, 829.

58 Y. H. Xu, P. Zeng, M. F. Li, J. Bian and F. Peng, *Sep. Purif. Technol.*, 2021, **279**, 1383–5866.

59 A. Zeb, *J. Food Biochem.*, 2020, **44**, e13394.

60 J. L. Espinoza-Acosta, P. I. Torres-Chávez, B. Ramírez-Wong, C. M. López-Saiz and B. Montaño-Leyva, *BioResources*, 2016, **11**, 5452–5481.

61 B. Wang, D. Sun, H. M. Wang, T. Q. Yuan and R. C. Sun, *ACS Sustainable Chem. Eng.*, 2019, **7**, 2658–2666.

62 Y. Qian, X. Zhong, Y. Li and X. Qiu, *Ind. Crops Prod.*, 2017, **101**, 54–60.

63 C. Frangville, M. Rutkevičius, A. P. Richter, O. D. Velev, S. D. Stoyanov and V. N. Paunov, *ChemPhysChem*, 2012, **13**, 4235–4243.

64 I. A. Gilca, V. I. Popa and C. Crestini, *Ultrason. Sonochem.*, 2015, **23**, 369–375.

65 F. M. C. Freitas, M. A. Cerqueira, C. Gonçalves, S. Azinheiro, A. Garrido-Maestu, A. A. Vicente, L. M. Pastrana, J. A. Teixeira and M. Michelin, *Int. J. Biol. Macromol.*, 2020, **163**, 1798–1809.



66 S. Paul, N. S. Thakur, S. Chandna, Y. N. Reddy and J. Bhaumik, *J. Mater. Chem. B*, 2021, **9**, 1592–1603.

67 M. Moradipour, E. K. Chase, M. A. Khan, S. O. Asare, B. C. Lynn, S. E. Rankin and B. L. Knutson, *Colloids Surf. B*, 2020, **191**, 111028.

68 M. N. Garcia Gonzalez, M. Levi, S. Turri and G. Griffini, *J. Appl. Polym. Sci.*, 2017, **134**, 45318.

69 A. G. Morena, A. Bassegoda, M. Natan, G. Jacobi, E. Banin and T. Tzanov, *ACS Appl. Mater. Interfaces*, 2022, **14**, 37270–37279.

70 W. Yang, E. Fortunati, D. Gao, G. M. Balestra, G. Giovanale, X. He, L. Torre, J. M. Kenny and D. Puglia, *ACS Sustainable Chem. Eng.*, 2018, **6**, 3502–3514.

71 W. Yang, H. Ding, G. Qi, J. Guo, F. Xu, C. Li, D. Puglia, J. Kenny and P. Ma, *Biomacromolecules*, 2021, **22**, 2693.

72 S. Kim, M. M. Fernandes, T. Matamá, A. Loureiro, A. C. Gomes and A. Cavaco-Paulo, *Colloids Surf. B*, 2013, **103**, 1–8.

73 T. Bruna, F. Maldonado-Bravo, P. Jara and N. Caro, *Int. J. Mol. Sci.*, 2021, **22**, 7202.

74 Q. ul A. Naqvi, A. Kanwal, S. Qaseem, M. Naeem, S. R. Ali, M. Shaffique and M. Maqbool, *J. Biol. Phys.*, 2019, **45**, 147–159.

75 S. Agnihotri, S. Mukherji and S. Mukherji, *RSC Adv.*, 2014, **4**, 3974–3983.

76 H. Akiyama, K. Fujii, O. Yamasaki, T. Oono and K. Iwatsuki, *J. Antimicrob. Chemother.*, 2001, **48**, 487–491.

77 A. Renzetti, J. W. Betts, K. Fukumoto and R. N. Rutherford, *Food Funct.*, 2020, **11**, 9370–9396.

78 R. Castaneda-Arriaga, A. Pérez-González, M. Reina, J. R. Alvarez-Idaboy and A. Galano, *J. Phys. Chem. B*, 2018, **122**, 6198–6214.

79 L. Panda and A. Duarte-Sierra, *Horticulturae*, 2022, **8**, 401.

80 A. Plaper, M. Golob, I. Hafner, M. Oblak, T. Šolmajer and R. Jerala, *Biochem. Biophys. Res. Commun.*, 2003, **306**, 530–536.

81 A. O. Gill and R. A. Holley, *Appl. Environ. Microbiol.*, 2004, **70**, 5750–5755.

82 N. Maldonado-Carmona, G. Marchand, N. Villandier, T. S. Ouk, M. M. Pereira, M. J. F. Calvete, C. A. Calliste, A. Žak, M. Pilksa, K. J. Pawlik, K. Matczyszyn and S. Leroy-Lhez, *Front. Microbiol.*, 2020, **11**, 606185.

83 I. Sondi and B. Salopek-Sondi, *J. Colloid Interface Sci.*, 2004, **275**, 177–182.

84 M. Danilczuk, A. Lund, J. Sadlo, H. Yamada and J. Michalik, *Spectrochim. Acta, Part A*, 2006, **63**, 189–191.

85 J. S. Kim, E. Kuk, K. N. Yu, J. H. Kim, S. J. Park, H. J. Lee, S. H. Kim, Y. K. Park, Y. H. Park, C. Y. Hwang, Y. K. Kim, Y. S. Lee, D. H. Jeong and M. H. Cho, *Nanomedicine*, 2007, **3**, 95–101.

86 L. Jaiswal, S. Shankar, J. W. Rhim and D. H. Hahm, *Int. J. Biol. Macromol.*, 2020, **159**, 859–869.

87 L. Zhang, H. Lu, J. Chu, J. Ma, Y. Fan, Z. Wang and Y. Ni, *ACS Sustainable Chem. Eng.*, 2020, **8**, 12655–12663.

88 A. Hamad, K. S. Khashan and A. Hadi, *J. Inorg. Organomet. Polym. Mater.*, 2020, **30**, 4811–4828.

89 Y. N. Slavin, K. Ivanova, J. Hoyo, I. Perelshtein, G. Owen, A. Haegert, Y.-Y. Lin, S. LeBihan, A. Gedanken, U. O. Häfeli, T. Tzanov and H. Bach, *ACS Appl. Mater. Interfaces*, 2021, **13**, 22098–22109.

90 Y. N. Slavin, K. Ivanova, W. L. Tang, T. Tzanov, S. D. Li and H. Bach, *Nanomaterials*, 2021, **11**, 1984.

91 R. G. Saratale, G. D. Saratale, G. Ghodake, S. K. Cho, A. Kadam, G. Kumar, B. H. Jeon, D. Pant, A. Bhatnagar and H. S. Shin, *Int. J. Biol. Macromol.*, 2019, **128**, 391–400.

92 R. G. Saratale, S. K. Cho, G. D. Saratale, A. A. Kadam, G. S. Ghodake, V. K. Magotra, M. Kumar, R. N. Bharagava, S. Varjani, R. R. Palem, S. I. Mulla, D. S. Kim and H. S. Shin, *Polymers*, 2022, **14**, 648.

93 D. Pletzer, J. Asnis, Y. N. Slavin, R. E. W. Hancock, H. Bach, K. Saatchi and U. O. Häfeli, *Int. J. Pharm.*, 2021, **596**, 120299.

94 M. B. Marulasiddeshwara, S. S. Dakshayani, M. N. Sharath Kumar, R. Chethana, P. Raghavendra Kumar and S. Devaraja, *Mater. Sci. Eng., C*, 2017, **81**, 182.

95 N. T. Tran, T. T. T. Nguyen, D. Ha, T. H. Nguyen, N. N. Nguyen, K. Baek, N. T. Nguyen, C. K. Tran, T. T. Van Tran, H. Van Le, D. M. Nguyen and D. Hoang, *Biomacromolecules*, 2021, **22**, 5327.

96 K. R. Aadil, N. Pandey, S. I. Mussatto and H. Jha, *J. Environ. Chem. Eng.*, 2019, **7**, 103296.

97 L. A. Zevallos Torres, A. L. Woiciechowski, V. Oliveira de Andrade Tanobe, A. Zandoná Filho, R. Alves de Freitas, M. D. Noseda, E. Saito Szameitat, C. Faulds, P. Coutinho, E. Bertrand and C. R. Soccol, *Int. J. Biol. Macromol.*, 2021, **167**, 1499–1507.

98 Y. Wang, Z. Li, D. Yang, X. Qiu, Y. Xie and X. Zhang, *J. Colloid Interface Sci.*, 2021, **583**, 80.

99 Y. Li, D. Yang, P. Li and Z. Li, *J. Mater. Res. Technol.*, 2022, **17**, 3211–3220.

100 D. M. Rocca, J. P. Vanegas, K. Fournier, M. C. Becerra, J. C. Scaiano and A. E. Lanterna, *RSC Adv.*, 2018, **8**, 40454–40463.

101 A. G. Morena, A. Bassegoda, J. Hoyo and T. Tzanov, *ACS Appl. Mater. Interfaces*, 2021, **13**, 14885–14893.

102 P. Li, W. Lv and S. Ai, *J. Exp. Nanosci.*, 2016, **11**, 18–27.

103 J. Hoyo, K. Ivanova, J. Torrent-Burgues and T. Tzanov, *Frontiers in Bioengineering and Biotechnology*, 2020, **8**, 439.

104 A. P. Richter, B. Bharti, H. B. Armstrong, J. S. Brown, D. Plemmons, V. N. Paunov, S. D. Stoyanov and O. D. Velev, *Langmuir*, 2016, **32**, 6468–6477.

105 C. E. Nix, B. J. Harper, C. G. Conner, A. P. Richter, O. D. Velev and S. L. Harper, *Antibiotics*, 2018, **7**, 40.

106 S. Gurunathan, J. W. Han, D. N. Kwon and J. H. Kim, *Nanoscale Res. Lett.*, 2014, **9**, 1–17.

107 I. P. Mukha, A. M. Eremenko, N. P. Smirnova, A. I. Mikhienkova, G. I. Korchak, V. F. Gorchev and A. Y. Chunikhin, *Appl. Biochem. Microbiol.*, 2013, **49**, 199–206.

108 N. Maldonado-Carmona, T. S. Ouk, N. Villandier, C. A. Calliste, M. J. F. Calvete, M. M. Pereira and S. Leroy-Lhez, *Antibiotics*, 2021, **10**, 513.

109 L. Chen, Y. Shi, B. Gao, Y. Zhao, Y. Jiang, Z. Zha, W. Xue and L. Gong, *ACS Sustainable Chem. Eng.*, 2020, **8**, 714–722.



110 L. M. Jose, S. Kuriakose and T. Mathew, *Photodiagn. Photodyn. Ther.*, 2021, **36**, 102479.

111 J. F. Zhong, L. Xu and X. L. Qin, *J. Compos. Mater.*, 2015, **49**, 2329–2335.

112 Q. F. Lü, J. Y. Zhang, J. Yang, Z. W. He, C. Q. Fang and Q. Lin, *Chem.-Eur. J.*, 2013, **19**, 10935–10944.

113 Ł. Kłapiszewski, T. Rzemieniecki, M. Krawczyk, D. Malina, M. Norman, J. Zdarta, I. Majchrzak, A. Dobrowolska, K. Czaczzyk and T. Jesionowski, *Colloids Surf., B*, 2015, **134**, 220–228.

114 A. P. Richter, J. S. Brown, B. Bharti, A. Wang, S. Gangwal, K. Houck, E. A. Cohen Hubal, V. N. Paunov, S. D. Stoyanov and O. D. Velev, *Nat. Nanotechnol.*, 2015, **10**, 817–823.

115 K. Lintinen, S. Luiro, P. Figueiredo, E. Sakarinen, Z. Mousavi, J. Seitsonen, G. N. S. Rivière, U. Mattinen, M. Niemelä, P. Tammela, M. Österberg, L. S. Johansson, J. Bobacka, H. A. Santos and M. A. Kostianen, *ACS Sustainable Chem. Eng.*, 2019, **7**, 15297–15303.

116 S. Paudel, J. Peña-Bahamonde, S. Shakiba, C. E. Astete, S. M. Louie, C. M. Sablivo and D. F. Rodrigues, *J. Hazard. Mater.*, 2021, **414**, 125454.

117 T. Zou, M. H. Sipponen and M. Österberg, *Front. Chem.*, 2019, **7**, 370.

118 T. E. Nypelö, C. A. Carrillo and O. J. Rojas, *Soft Matter*, 2015, **11**, 2046–2054.

119 B. M. Amos-Tautua, S. P. Songca and O. S. Oluwafemi, *Molecules*, 2019, **24**, 2456.

120 C. Jiménez-González, D. J. C. Constable and C. S. Ponder, *Chem. Soc. Rev.*, 2012, **41**, 1485–1498.

121 M. Ahamed, M. S. AlSalhi and M. K. J. Siddiqui, *Clin. Chim. Acta*, 2010, **411**, 1841–1848.

122 J. Dobias and R. Bernier-Latmani, *Environ. Sci. Technol.*, 2013, **47**, 4140–4146.

123 Y. Li and E. Cummins, *J. Environ. Sci. Health, Part A: Toxic/Hazard. Subst. Environ. Eng.*, 2020, **55**, 704–725.

124 B. Cunningham, A. E. Engstrom, B. J. Harper, S. L. Harper and M. R. Mackiewicz, *Nanomaterials*, 2021, **11**, 1516.

125 L. I. Tolosa, A. J. Rodríguez-Malaver, A. M. González and O. J. Rojas, *J. Colloid Interface Sci.*, 2006, **294**, 182–186.

126 L. B. Brenelli, L. R. B. Mariutti, R. Villares Portugal, M. A. de Farias, N. Bragagnolo, A. Z. Mercadante, T. T. Franco, S. C. Rabelo and F. M. Squina, *Ind. Crops Prod.*, 2021, **167**, 113532.

127 S. U. Pickering, *J. Chem. Soc., Trans.*, 1907, **91**, 2001–2021.

128 L. A. M. Nevrez, L. B. Casarrubias, A. Celzard, V. Fierro, V. T. Müoz, A. C. Davila, J. R. T. Lubian and G. G. Snchez, *Sci. Technol. Adv. Mater.*, 2011, **12**, 45006–45022.

129 Y. Y. Wang, X. Meng, Y. Pu and A. J. Ragauskas, *Polymers*, 2020, **12**, 2277.

130 S. Pérez-Rafael, K. Ivanova, I. Stefanov, J. Puiggallí, L. J. del Valle, K. Todorova, P. Dimitrov, D. Hinojosa-Caballero and T. Tzanov, *Acta Biomater.*, 2021, **134**, 131–143.

131 E. Gerbin, G. N. Rivière, L. Foulon, Y. M. Frapart, B. Cottyn, M. Pernes, C. Marcuello, B. Godon, A. Gainvors-Claisse, D. Crônier, A. Majira, M. Österberg, B. Kurek, S. Baumberger and V. Aguié-Béghin, *Int. J. Biol. Macromol.*, 2021, **181**, 136.

132 X. Zhang, W. Liu, D. Sun, J. Huang, X. Qiu, Z. Li and X. Wu, *ChemSusChem*, 2020, **13**, 4974.

133 A. G. Morena, I. Stefanov, K. Ivanova, S. Pérez-Rafael, M. Sánchez-Soto and T. Tzanov, *Ind. Eng. Chem. Res.*, 2020, **59**, 4504–4514.

134 S. Li, Y. Zhang, X. Ma, S. Qiu, J. Chen, G. Lu, Z. Jia, J. Zhu, Q. Yang, J. Chen and Y. Wei, *Biomacromolecules*, 2022, **23**, 1622–1632.

135 M. Li, X. Jiang, D. Wang, Z. Xu and M. Yang, *Colloids Surf., B*, 2019, **177**, 370–376.

136 P. Deng, F. Chen, H. Zhang, Y. Chen and J. Zhou, *ACS Appl. Mater. Interfaces*, 2021, **13**, 52333–52345.

137 M. K. Haider, A. Ullah, M. N. Sarwar, Y. Saito, L. Sun, S. Park and I. S. Kim, *Int. J. Biol. Macromol.*, 2021, **173**, 315–326.

138 World Health Organization, *Health and Food Safety - 2015 Annual Activity Report*, 2016.

139 A. Jayakumar, S. Radoor, J. T. Kim, J. W. Rhim, J. Parameswaranpillai and S. Siengchin, in *Bionanocomposites for Food Packaging Applications*, Woodhead Publishing, 2022, pp. 323–337.

140 W. Yang, J. S. Owczarek, E. Fortunati, M. Kozanecki, A. Mazzaglia, G. M. Balestra, J. M. Kenny, L. Torre and D. Puglia, *Ind. Crops Prod.*, 2016, **94**, 800–811.

141 W. Yang, E. Fortunati, F. Dominici, G. Giovanale, A. Mazzaglia, G. M. Balestra, J. M. Kenny and D. Puglia, *Eur. Polym. J.*, 2016, **79**, 1–12.

142 X. Wang, S. Wang, W. Liu, S. Wang, L. Zhang, R. Sang, Q. Hou and J. Li, *Carbohydr. Polym.*, 2019, **225**, 115213.

143 E. Lizundia, I. Armentano, F. Luzi, F. Bertoglio, E. Restivo, L. Visai, L. Torre and D. Puglia, *ACS Appl. Bio Mater.*, 2020, **3**, 5263.

144 L. Deng, C. Cai, Y. Huang, Y. Dong and Y. Fu, *Int. J. Biol. Macromol.*, 2021, **185**, 513–524.

145 S. Hu and Y. Lo Hsieh, *Carbohydr. Polym.*, 2015, **131**, 134.

146 S. Shankar and J. W. Rhim, *Food Hydrocolloids*, 2017, **71**, 76–84.

147 S. Shankar, J. W. Rhim and K. Won, *Int. J. Biol. Macromol.*, 2018, **107**, 1724.

148 E. Lizundia, J. L. Vilas, A. Sangroniz and A. Etxeberria, *Eur. Polym. J.*, 2017, **91**, 10–20.

149 C. Lambré, J. M. Barat Bavier, C. Bolognesi, A. Chesson, P. S. Cocconcelli, R. Crebelli, D. M. Gott, K. Grob, E. Lampi, M. Mengelers, A. Mortensen, I. L. Steffensen, C. Tlustos, H. Van Loveren, L. Vernis, H. Zorn, L. Castle, E. Di Consiglio, R. Franz, N. Hellwig, S. Merkel, M. R. Milana, E. Barthélémy and G. Rivière, *EFSA J.*, 2021, **19**.

150 E. Capecchi, D. Piccinino, E. Tomaino, B. M. Bizzarri, F. Polli, R. Antiochia, F. Mazzei and R. Saladino, *RSC Adv.*, 2020, **10**, 29031–29042.

151 M. K. Riley and W. Vermerris, *Materials*, 2022, **15**, 303.

152 S. Ma, X. Feng, F. Liu, B. Wang, H. Zhang and X. Niu, *Eng. Life Sci.*, 2021, **21**, 709–720.



153 W. Yang, E. Fortunati, F. Bertoglio, J. S. Owczarek, G. Bruni, M. Kozanecki, J. M. Kenny, L. Torre, L. Visai and D. Puglia, *Carbohydr. Polym.*, 2018, **181**, 275–284.

154 A. I. Visan, G. Popescu-Pelin, O. Gherasim, V. Grumezescu, M. Socol, I. Zgura, C. Florica, R. C. Popescu, D. Savu, A. M. Holban, R. Cristescu, C. E. Matei and G. Socol, *Polymers*, 2019, **11**, 283.

155 X. He, Z. Li, J. Li, D. Mishra, Y. Ren, I. Gates, J. Hu and Q. Lu, *Small*, 2021, **17**, 2103521.

156 H. Wang, J. Xu, K. Li, Y. Dong, Z. Du and S. Wang, *J. Mater. Chem. B*, 2022, **10**, 1301–1307.

157 X. Han, Y. Zhang, F. Ran, C. Li, L. Dai, H. Li, F. Yu, C. Zheng and C. Si, *Ind. Crops Prod.*, 2022, **176**, 114366.

158 D. Gan, W. Xing, L. Jiang, J. Fang, C. Zhao, F. Ren, L. Fang, K. Wang and X. Lu, *Nat. Commun.*, 2019, **10**, 1487.

159 P. Deng, F. Chen, H. Zhang, Y. Chen and J. Zhou, *ACS Appl. Mater. Interfaces*, 2021, **13**, 52333.

160 W. Yang, F. Xu, X. Ma, J. Guo, C. Li, S. Shen, D. Puglia, J. Chen, P. Xu, J. Kenny and P. Ma, *Mater. Sci. Eng., C*, 2021, **129**, 112385.

161 S. Chandna, N. S. Thakur, R. Kaur and J. Bhaumik, *Biomacromolecules*, 2020, **21**, 3216.

162 M. Li, X. Jiang, D. Wang, Z. Xu and M. Yang, *Colloids Surf., B*, 2019, **177**, 370–376.

163 K. R. Aadil, S. I. Mussatto and H. Jha, *Int. J. Biol. Macromol.*, 2018, **120**, 763–767.

164 M. K. Haider, A. Ullah, M. N. Sarwar, T. Yamaguchi, Q. Wang, S. Ullah, S. Park and I. S. Kim, *Polymers*, 2021, **13**, 748.

165 B. Ying and X. Liu, *iScience*, 2021, **24**, 103174.

166 Q. Zeng, X. Qi, G. Shi, M. Zhang and H. Haick, *ACS Nano*, 2022, **16**, 1708–1733.

167 S. Hamdan, I. Pastar, S. Drakulich, E. Dikici, M. Tomic-Canic, S. Deo and S. Daunert, *ACS Cent. Sci.*, 2017, **3**, 163–175.

168 J. Domínguez-Robles, Á. Cárcamo-Martínez, S. A. Stewart, R. F. Donnelly, E. Larrañeta and M. Borrega, *Sustainable Chem. Pharm.*, 2020, **18**, 2352–5541.

169 R. Foulkes, E. Man, J. Thind, S. Yeung, A. Joy and C. Hoskins, *Biomater. Sci.*, 2020, **8**, 4653–4664.

